

INVESTIGATION OF SHEAR BEHAVIOUR OF SLENDER BEAMS USING FINITE ELEMENT ANALYSIS



FINAL YEAR PROJECT UG BE CE 2011

By

Usman Mahmood
Asad Ullah Malik
Aakif Saeed Iqbal
Faizan Hameed

Project Advisor: Dr. Wasim Khaliq

**NUST Institute of Civil Engineering
School of Civil and Environmental Engineering
National University of Sciences and Technology, Islamabad, Pakistan**

2015

This is to certify that the
Final Year Project Titled
**INVESTIGATION OF SHEAR BEHAVIOUR OF SLENDER
BEAMS USING FINITE ELEMENT ANALYSIS**

Submitted by

Usman Mahmood	2011-NUST-SCEE-BE-CE-119
Aakif Saeed Iqbal	2011-NUST-SCEE-BE-CE-01
Asad Ullah Malik	2011-NUST-SCEE-BE-CE-16
Faizan Hameed	2011-NUST-SCEE-BE-CE-41

has been accepted towards the requirements
for the undergraduate degree

in

CIVIL ENGINEERING

Dr. Wasim Khaliq
Associate Professor
NUST Institute of Civil Engineering
School of Civil and Environmental Engineering
National University of Sciences and Technology, Islamabad, Pakistan

**DEDICATED TO THE OUR PARENTS AND MARTYRS OF
APS PESHAWAR**

ACKNOWLEDGEMENTS

Firstly we would like to thank Almighty Allah, without Whose divine guidance we were ignorant. Our sincere gratitude to our supervisor, Dr. Wasim Khaliq, who believed in us and agreed to work with us in the first place. It was his patience, vision, supportiveness and depth of knowledge which presented itself as a role model for us to follow. His diligence, compassion and cooperation was our key to success. We feel privileged to work under him and thank him with all our heart.

We would also like to thank Dr. Amir Mubashir (SMME) who helped us and supported us at every moment. His depth of knowledge of the subject proved very vital for us and provided coherent answers to our endless questions.

We would like to acknowledge our friends & family who supported us at every moment. They encouraged us for choosing this project and shared our passion to pursue our dreams. Lastly we would like to thank School of Civil & Environmental Engineering for providing us the necessary resources for successful project execution.

ABSTRACT

Reinforced concrete (RC) beams may not be able to utilize their maximum flexural strength in the absence of adequate shear reinforcement. While ACI code specifies minimum amount of shear reinforcement in RC beams, the established formulae do not cover all parameters associated with shear strength of RC beams and result in conservative design. Zararis (2003), proposed the empirical formula which incorporates additional factors in calculation of shear strength. This formula yields less conservative yet equally reliable results in terms of shear strength in RC beams. In this project, formulae provided by Zararis (2003) and Kashif (2014) were studied through analytical models using commercial software ABAQUS®, and validated for experimentally tested concrete slender beams with varying amounts of shear reinforcement. Non-linear finite element analysis was carried out to measure the load-displacement behavior and the cracking characteristics in RC beams. The analysis employed a concrete damage plasticity model in ABAQUS software. The parametric analysis was carried out by varying the shear span to depth ratio and the amounts of shear and longitudinal reinforcement in RC beams were kept as same as in the benchmark analysis. Additionally, the sensitivity of results were investigated against the minimum shear reinforcement provisions provided by ACI, Zararis and Papadakis (2001), Zararis (2003) and Kashif (2014). Lastly, an equation for minimum amount of shear reinforcement to attain full flexure capacity has been proposed.

TABLE OF CONTENTS

TABLE OF CONTENTS	vi
LIST OF TABLES	x
LIST OF FIGURES	xi
KEY TO SYMBOLS OR ABBREVIATIONS	xiii
<u>CHAPTER 1</u>	1
INTRODUCTION	1
1.1 General	1
1.2 Developments in Shear Design	2
1.3 Significance of Shear	4
1.4 Scope	5
1.5 Objectives.....	5
<u>CHAPTER 2</u>	6
LITERATURE REVIEW	6
2.1 Basic Shear Concepts	6
2.1.1 Shear Strength of Concrete.....	6
2.1.2 Importance of Shear Reinforcement.....	7
2.2 Shear Transfer Mechanism.....	8
2.2.1 Beam Action	9
2.2.2 Arch Action	9
2.2.3 Model for Flexure-Shear Interaction	10
2.3 Primary Mechanisms of Shear Resistance	11
2.4 Classification of Beams.....	12
2.5 Prediction of Shear behavior	12
2.6 Failure Modes in Shear	13
2.6.1 Diagonal Tension Failure	15
2.6.2 Shear Tension Failure.....	15

2.6.3 Shear Compression Failure.....	15
2.6.4 Flexural Failure.....	15
2.6.5 Anchorage Failure	16
2.6.6 Bearing Failure	16
2.7 Parameters influencing shear strength.....	16
2.7.1 Shear Span-to-Depth Ratio (a/d)	17
2.7.2 Depth of Members or Size Effect.....	18
2.7.3 Axial Force	18
2.7.4 Concrete Tensile Strength	18
2.8 Shear Theories.....	19
2.8.1 Shear Stresses in Un-cracked Beams.....	19
2.8.2 Comb Model by Kani	20
2.9 ACI Prediction of Minimum Shear Reinforcement	21
2.10 Zararis Theory of Critical Shear Crack.....	22
2.10.1 Shear Strength of Beams without Transverse Reinforcement.....	22
2.10.2 Shear Failure Mechanism in Beams with Transverse Reinforcement.....	23
2.10.3 Zararis’s minimum Shear Reinforcement.....	24
2.10.4 Experimental Verification	25
2.11 Shear behavior of Normal Strength Concrete Slender Beams	26
2.12 Fracture Mechanics	27
2.13 Numerical Modeling of Concrete.....	27
2.13.1 Discrete Crack Approach.....	27
2.13.2 Smeared Crack Approach.....	27
2.13.3 Cohesive crack Model	28
<u>CHAPTER 3</u>	30
RESEARCH METHODOLOGY	30
3.1 Methodology	30
3.1.1 Benchmark Analysis.....	30
3.1.2 Parametric Analysis.....	30

3.2 Simulation Specifications.....	32
3.3 Software Model	32
3.3.1 Beam Solid Model	32
3.3.2 Steel Truss model	33
3.3.3 Displacement control deflection.....	33
3.3.4 Analytical rigid node/ surface.....	34
3.3.5 Material Model	34
3.3.6 Concrete Material Input Properties.....	36
3.4 Simulation in ABAQUS (FEM software)	39
3.4.1 Parts definition.....	39
3.4.2 Material definition	39
3.4.3 Section assignment	40
3.4.4 Assembly/ Interaction.....	40
3.4.5 Meshing	40
3.4.6 Step formation	40
3.4.7 Loading/ Boundary Conditions	40
3.4.8 Field Output.....	41
3.4.9 Visualization.....	41
<u>CHAPTER 4</u>	42
MODELLING RESULTS	42
4.1 Choice of Mesh Size	42
4.2 Effect of dilation angle Ψ and Viscosity Coefficient ν for material calibration.....	43
4.3 Determination of Shear Strength (V_u) of the concrete beam for all sections	44
4.4 Load-Displacement characteristics of experimental verses the FEM results.....	45
<u>CHAPTER 5</u>	53
ANALYSIS AND INTERPRETATION OF RESULTS	53
5.1 Comparison of ultimate shear strength predicted by ACI and FEM.....	54
5.2 Cracking Pattern of the modelled beams.....	59

5.2.1 General Cracking Pattern.....	59
5.3 Beams with Shear Span to Depth Ratio 2.5	60
5.4 Beams with Shear Span to Depth Ratio 3.0	62
5.5 Beams with Shear Span to Depth Ratio of 3.5	63
5.6 Beams with Shear Span to Depth Ratio of 4.0.....	64
CHAPTER 6	65
DERIVATION OF MODIFIED EQUATIONS	65
6.1 Equations for Ultimate Shear Strength and Minimum Shear Reinforcement	65
6.2 Derivation of Minimum Shear Reinforcement which ascertains full flexure capacity	66
CHAPTER 7	68
CONCLUSIONS AND RECOMMENDATION	68
7.1 Conclusions	68
7.3 Recommendations	68
APPENDIX	69
BIBLIOGRAPHY	77

LIST OF TABLES

Table 2.1: Failure Modes in Shear	14
Table 2.2: Factors affecting Shear Strength	17
Table 2.3: Comparisons of experimental and theoretical results of 174 beams.....	26
Table 2.4: Kashif (2014) experimental program.....	26
Table 3.1: Summary of the beams modelled in ABAQUS.	31
Table 3.2: ABQUS/Standard settings for the analysis	32
Table 4.1: Error with Dilation angle and Viscosity parameter variance	43
Table 5.1: Specifications of N, A, Z and M series beams.....	53
Table 5.2: Experimental Comparison of results between (Kashif, 2014) and ABAQUS (FEM) for shear span-to-depth ratio of 2.5	54
Table 5.3: Comparison of results between ACI and ABAQUS (FEM) for shear	55
span-to-depth ratio of 3	55
Table 5.4: Comparison of results between ACI and ABAQUS (FEM) for shear	55
span-to-depth ratio of 3.5	55
Table 5.5: Comparison of results between ACI and ABAQUS (FEM) for shear	56
span-to-depth ratio of 4.0	56
Table 5.6: Comparison of results of Shear Strength predicted between ACI and modified equation.....	57
Table 1: Beam N1 Experimental and FEM Model’s Load Deflection Comparison	69
Table 2: Beam N2 Experimental and FEM Model’s Load Deflection comparison.....	70
Table 3: Beam A1 Experimental and FEM Model’s Load Deflection comparison.....	71
Table 4: Beam A2 Experimental and FEM Model’s Load Deflection comparison.....	72
Table 5: Beam Z1 Experimental and FEM Model’s Load Deflection comparison	73
Table 6: Beam Z2 Experimental and FEM Model’s Load Deflection comparison	74
Table 7: Beam M1 Experimental and FEM Model’s Load Deflection comparison	75
Table 8: Beam M2 Experimental and FEM Model’s Load Deflection comparison	76

LIST OF FIGURES

Figure 2.1: Resisting Moment and Shear in response to external loads	6
Figure 2.2: Transverse and Inclined Stirrups	7
Figure 2.3: Forces and Moments across a cracked concrete section	8
Figure 2.4: Arch action mechanism	10
Figure 2.5: Flexure Shear Interaction	11
Figure 2.6: Internal forces developed across an inclined crack	12
Figure 2.7: Principle Stress Trajectory	13
Figure 2.8: Distribution of Shear Stresses for un-cracked rectangular beam	20
Figure 2.9: Relation between Cohesive Stress and Crack Opening Width.....	29
Figure 2.10: Hierarchy diagram of Concrete Cracking Model (Hofstetter and Mesch) ..	29
Fig.3.1: Concrete Compression Damage	36
Fig.3.2: Concrete Tension Damage	37
Fig-4.1: Stabilization of U2 with the increase in element number	42
Fig 4.2: Effect of dilation angle and viscosity parameter on the load-displacement.....	43
Fig 4.3: Shear Stresses along the three planes plotted verses step time	44
Figure 4.4: A1 Beam Load vs. Deflection at midpoint.....	45
Figure 4.5: A1 Beam Load vs. Deflection at quarter points	45
Figure 4.6: A2 Beam Load vs. Deflection at midpoint.....	46
Figure 4.7: A2 Beam Load vs Deflection at quarter points	46
Figure 4.8: N1 Beam Load vs. Deflection at midpoint.....	47
Figure 4.9: N1 Beam Load vs. Deflection at quarter points	47
Figure 4.10: N2 Beam Load vs. deflection at midpoint.....	48
Figure 4.11: N2 Beam Load vs. deflection at quarter points	48
Figure 4.12: Z1 Beam Load vs. Displacement at midpoint	49
Figure 4.13: Z1 Beam Load vs. Deflection at quarter points.....	49
Figure 4.14: Z2 Beam Load vs. Deflection at quarter points.....	50
Figure 4.15: Z2 Beam Load vs. Deflection at midpoint	50
Figure 4.16: M1 Beam Load vs. Deflection at quarter points.....	51
Figure 4.17: M1 Beam Load vs. Deflection at midpoint	51
Figure 4.18: M2 Beam Load vs. Deflection at quarter points.....	52
Figure 4.19: M2 Beam Load vs. Deflection at midpoint	52
Fig 5.1: Change in RSSV and its trend with increasing a/d ratio	56
Figure 5.2: Improved results of the modified equation as compared to ACI.....	58

Figure 5.3: The variation in value of α with the increase in a/d ratio.....	59
Fig 5.4: Inclined Cracking for Beam N1 with $a/d = 2.5$	60
Fig 5.5: Inclined cracking for Beam N2 with $a/d = 2.5$	60
Fig 5.6: Lesser flexure cracks appear for Beam A1 with $a/d = 2.5$	60
Fig 5.7: Lesser flexure cracks appear for Beam A2 with $a/d = 2.5$	60
Fig 5.8: Both flexure and shear cracks appear for Beam Z1 with $a/d = 2.5$	61
Fig 5.9: Both flexure and shear cracks appear for Beam Z2 with $a/d = 2.5$	61
Fig 5.10: Flexure cracks and inclined cracks for Beam M1 with $a/d 2.5$	61
Fig 5.11: Flexure cracks and inclined cracks for Beam M2 with $a/d 2.5$	61
Fig 5.12: Flexure cracks and inclined cracks for Beam N3 with $a/d 3.0$	62
Fig 5.13: Flexure cracks and inclined cracks for Beam A3 with $a/d 3.0$	62
Fig 5.14: Flexure cracks and inclined cracks for Beam Z3 with $a/d 3.0$	62
Fig 5.15: Flexure cracks and inclined cracks for Beam M3 with $a/d 3.0$	62
Fig 5.16: Flexure cracks and inclined cracks for Beam N4 with a/d of 3.5	63
Fig 5.17: Flexure cracks and inclined cracks for Beam A4 with a/d of 3.5	63
Fig 5.18: Flexure cracks and inclined cracks for Beam Z4 with a/d of 3.5	63
Fig 5.19: Flexure cracks and inclined cracks for Beam M4 with a/d of 3.5	63
Fig 5.20: Flexure cracks and shear inclined cracks for Beam N5 with a/d of 4.0	64
Fig 5.21: More Flexural cracks for Beam A5 with a/d of 4.0	64
Fig 5.22: Flexure and inclined cracks for Beam Z5 with a/d of 4.0	64
Fig 5.23: Flexure cracks for Beam M5 with a/d of 4.0	64
Figure 6.1: Relation of %Nominal Capacity to Transverse Reinforcement Ratio.....	67

KEY TO SYMBOLS OR ABBREVIATIONS

$\frac{a}{d}$	= shear span to depth ratio
ρ_l	= longitudinal reinforcement ratio
ρ_v	= transverse reinforcement ratio
f'_c	= compressive strength of concrete (28 days)
f_{yt}	= yield strength of transverse reinforcement
f_{ct}	= tensile splitting strength of concrete
T	= tensile force
C	= compressive force
Jd	= moment arm
l_d	= development length
f_1	= principle tensile stress
f_2	= principle compressive stress
ε_2	= principle compressive strain
ε_1	= principle tensile strain
w	= crack opening width
V_b	= shear flow across horizontal plane
V_u	= shear force at shear failure
V_{cr}	= shear force at the beginning of cracking of the second branch
v_{cr}	= shear stress at the beginning of cracking of the second branch
V_{ccr}	= shear resistance in the compression region of concrete
V_s	= force of stirrups along the critical diagonal crack
V_d	= shear force of bars of main reinforcement
NSC	= normal strength concrete
HSC	= high strength concrete
FEA	= finite element analysis
MCFT	= modified compression field theory

CHAPTER 1

INTRODUCTION

1.1 General

Over the decades the phenomena of shear failure in structural members have been a matter of pure speculation for the concrete specialists. Various attempts that aim to provide a rigorous solution are either based on deterministic mechanical assumptions which unfortunately did not take into account many factors of uncertainty or were derived from empirical tests obtained from extensive lab testing. These methods are meticulously not accurate but provide a reliable prediction to model the structures within a band of uncertainty involved.

Behavior of slender beams subjected to various types of loadings has been studied through a number of experimental and simulation programs. Consensus over a single theory to predict the response of members under shear does not exist even after extensive research efforts. Members may fail in shear before attaining its nominal flexural capacity. This is a highly undesirable phenomenon since the shear failures are generally brittle and unexpected. This makes it imperative to have an in depth understanding of the shear behavior of reinforced concrete beams.

Researchers have identified a large number of factors which influence both the shear behavior and the minimum amount of shear reinforcement required in the beams. However, it is felt that these factors have not so far been fully incorporated in the ACI code provisions for shear. As a result, the current provisions are still based on semi empirical considerations

1.2 Developments in Shear Design

The intriguing mechanism of shear and its behavior in reinforced concrete members has led to many debates and suppositions. This topic paved way to significant amount of researches particularly the last six decades has witnessed a substantial rise in its in depth study.

Mörsch (1910), one of the early notables, predicted shear behavior over the cross section of a reinforced concrete beam with flexural cracks. After rigorous study, he concluded that the shear stress has a constant value from bottom to neutral axis and then varies until it reaches the top surface fiber. He also stated that shear stresses can be calculated by using simple equilibrium relationships if the flexural stresses at different longitudinal sections of a beam are known. Mörsch (1910) and Ritter (1899) are the pioneers that introduced the Truss Model which was followed for many years; this model neglected concrete's contribution to shear resistance.

Talbot, with his most prominent contribution to experimental study, successfully tested 188 beams under shear loading. In 1907, he stated:

“...with this number of tests, one would expect the understanding of the problem to be quite complete. However, this is not the case, there is still much to be learned before the problems may be considered solved”

(Talbot 1909)

Universities across the globe played a vital role and made efforts in understanding the complex nature of shear. The noteworthy institutes among them were Universities of Illinois, Toronto and Stuttgart; which were primarily involved in publishing considerable quantity of research papers on the subject. American Concrete Institute (ACI) drafted its shear provisions for the ACI 318 Code based on rigorous experiments and research data but an unfortunate collapse of two US Air Force warehouses in 1955 meant critical

amendments in the ACI Code were absolutely necessary. The beams in these warehouses failed under dead load only, when subjected to a shear stress of 0.5 MPa, whereas ACI code allowed a working shear stress of 0.62 MPa. The dramatic incident led to serious changes in design practice, among them was the provision of minimum web reinforcement. Moreover, it instigated extensive research in attempts to explain how shear is transmitted in cracked reinforced concrete beams. MacGregor, Wight et al. (1997), explained shear force in terms of Beam and Arch Action.

Kani (1964), hailing from University of Toronto, is highly notable for his extensive experimental research. He was the pioneer who systematically studied shear behavior with respect to compressive strength (f'_c), longitudinal reinforcement (ρ_l) and shear span to depth ratio (a/d). He experimented with large number of rectangular beams after which he classified them into very short, short, slender and very slender beams. His famous contribution named "*Kani's Valley of Shear Failures*" incorporated a relationship between a/d ratio, shear capacity and reinforcement ratio. His highly regarded theory of diagonal failure stated that it's influenced by strength and ratio of steel, shape of section, strength of concrete, shear arm ratio, type and detailing of web reinforcement, pre-stressed conditions and direction of loading.

Many researchers have considered the span to depth ratio as a significant parameter for defining shear strength of a beam. This is evident from the Joint ASCE-ACI several committees and proceeding reports which tries to explain the complex concept by means of equations and most importantly ACI-318-11 Code specifies equation (11-5) denotes shear strength of concrete (V_c) as a functions of a/d ratio and longitudinal reinforcement ratio (ρ_l).

Zararis and Papadakis (2001), postulated a hypothetical theory based on an in depth study of the mechanism of critical cracks which leads to failure of beams. His theory has gained considerable attention for the fact that equations which justify this hypothesis have been developed and these conform to both, ACI and Eurocode. It has been claimed that the equations yield results which are reliable and far more accurate in predicting the shear capacity of slender beams. Zararis (2003) other contribution is the relationship between

shear reinforcement (ρ_v) longitudinal reinforcement ratio (ρ_l) and shear span to depth ratio (a/d) for which he has devised an equation for minimum shear reinforcement.

Kashif Shehzad (2014), a post-graduate of NUST, carried out his research which was an extension to the theory proposed by Zararis and Papadakis (2001) and Zararis (2003). His experimental research led to not only validating Zararis theory but he proposed a modified equation by incorporating a new factor; development length (l_d) which was missing in prior work. His experimental results proved that the modified equation is more accurate as compared to previous work.

1.3 Significance of Shear

Tensile reinforcement makes the beam stronger against flexure and the failure that occurs is tensile in nature that gives ample amount of time and warning along with the time for corrective measures before failure (in the form of spalling of concrete and abnormal deflections). But there are other factors that need to be accounted for the beam design like shear.

The shear failure whereas is predominantly brittle in nature. It is difficult to predict accurately and if the beam is overloaded till failure, then this failure occurs suddenly without any warning causing catastrophic damage.

Economy of design demands, in most cases, that beams must be capable of developing its full flexure (moment) capacity rather than having its strength limited by premature shear failure. This reduces the chances of sudden and explosive shear failure, giving warning of impending distress. Therefore if a large safety margin relative to available shear strength of the beam doesn't exist, special shear reinforcement, known as web reinforcement is used to increase the strength.

1.4 Scope

The scope of this project is to study the shear behavior of reinforced concrete slender beams using Finite Element Modeling. The aim is to analyze the formula provided by Zararis and Papadakis (2001), Zararis (2003), (Kashif Shehzad 2014); which postulates shear failure by the formation of shear critical cracks. This analysis is performed through analytical models using a commercial software ABAQUS®, and validating it for experimentally tested concrete slender beams with varying amounts of shear reinforcement. ACI Code provisions on shear have been devised based on years of thorough research and extensive experimental results yet it does not incorporate all the factors which contribute to shear strength of slender concrete. Zararis's and Kashif's equation however takes into account all important factors which are believed to influence shear strength and yield accurate results. Yet an equation with closer prediction of minimum shear requirement is proposed.

1.5 Objectives

The objectives of the project are to:-

- Determine the accuracy of prevalent expressions for predicting the ultimate shear capacity of RC beams.
- Establish minimum shear reinforcement requirement in RC beams incorporating additional factors which affect the shear behavior.
- Predicting cracking behavior graphically using FEM.

LITERATURE REVIEW

2.1 Basic Shear Concepts

2.1.1 Shear Strength of Concrete

Beams resist loads by means of internal moments (M) and shear (V) as indicated in Figure (2.1). Shear forces should be considered, as they lead to diagonal cracking, if the moments are not constant over its length. These cracks can cause an undesired abrupt failure causing the member to fail prematurely. Therefore, properly calculated quantities longitudinal and transverse reinforcement must be provided to avoid such failure.

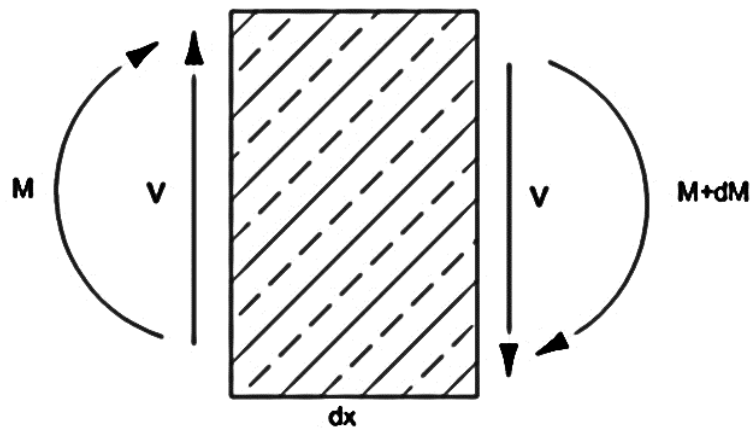


Figure 2.1: Resisting Moment and Shear in response to external loads

Determination of flexure strength is based on Hook’s Law whereas for the shear strength, there are two cases discussed as follows:-

Beams without Shear Reinforcement:

In the absence of shear reinforcement, only shear transfer mechanism provides the requisite shear resistance, as explained later in Section 2.2. This primarily is the point where codes of practice lack a theory and use totally empirical procedures. (Collins, Bentz et al. 2008).

Beams with Shear Reinforcement

When stirrups or shear reinforcement is provided to the beams; their shear resistance can be best ascertained using the truss analogy developed by Ritter and Morsch.

2.1.2 Importance of Shear Reinforcement

The main purpose of shear reinforcement is to seize the development of the diagonal tension cracking. Generally, the design of shear reinforcement is in a manner so that the inclined cracks shall cross two stirrups with specified spacing in between. It is pertinent to mention that the spacing of shear reinforcement design is affected by the change in shear force as it varies along the length of the beam. It is recommended to use transverse stirrups over inclined stirrups as shown in Figure (2.2).

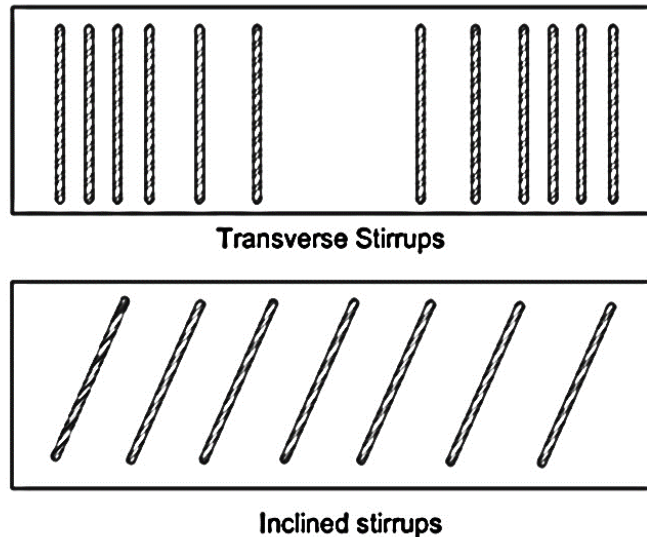


Figure 2.2: Transverse and Inclined Stirrups.
Transverse Stirrups perform better in stress reversals

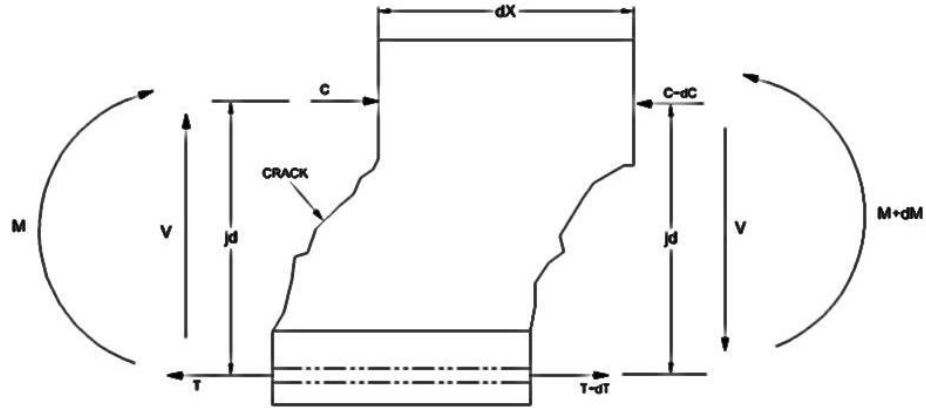


Figure 2.3: Forces and Moments across a cracked concrete section

It is because the inclined stirrups are not as effective in beams resisting shear reversals i.e. seismic loads, as the reversals will cause cracking parallel to inclined reinforcement rendering it ineffective.

2.2 Shear Transfer Mechanism

In RC beams, two load transfer mechanism dictates the transfer of shear; known as the beam *action* and *arch action*. Both these actions depend on shear span to depth ratio (a/d ratio). In order to mathematically express these shear transfer mechanisms, consider a free body diagram of the portion of a RC beam between two cracks as shown in Figure (2.3).

Shear force (V) is related to the tensile force in the bar (T) as:

$$V = \frac{d}{dx}(T \times Jd)$$

$$V = Jd \frac{d}{dx}(T) + T \frac{d}{dx}(Jd)$$

2.2.1 Beam Action

In slender beams where a/d ratio is greater than 2.5, shear is transferred primarily by beam action. In this mechanism, the lever arm (Jd) remains constant and the shear force is transferred in beam action as follows:

$$\frac{d(Jd)}{dx} = 0 \text{ and } V = \frac{d(T)}{dx}(Jd)$$

$$\frac{d(Jd)}{dx} = 0 \quad \text{and} \quad V = \frac{d(T)}{dx}(Jd)$$

Where, $V_b = \frac{d(T)}{dx}$ is the shear flow across any horizontal plane between the reinforcement and compression zone. For beam action to exist shear flow must be present.

2.2.2 Arch Action

It is a force transfer mechanism for those beams where shear span to depth ratio a/d ratio is less than 2.5. Beams in this category are known as *deep beams*. This generally gives more strength to the member, which can withstand considerably more load than at shear cracking

Russo and Zingone (1991), in their study, concluded that shear-compression failure is the result of arch action and beam action leads to diagonal tension (discussed later).

On the other hand if the shear flow; $\frac{d(T)}{dx}$ equals zero, then the shear force is transferred by arch action as follows:

$$V = T \frac{d(Jd)}{dx}$$

It may be argued that the shear span to depth ratio (a/d) is what effects the shear resistance because the applied shear force may be transmitted directly to the supports by means of compressive struts (arch action) of the concrete. In this kind of member, compressive force are formed in the inclined strut and the longitudinal reinforcement transmit tension force T which are constant over the length of shear span as shown in Figure (2.4).

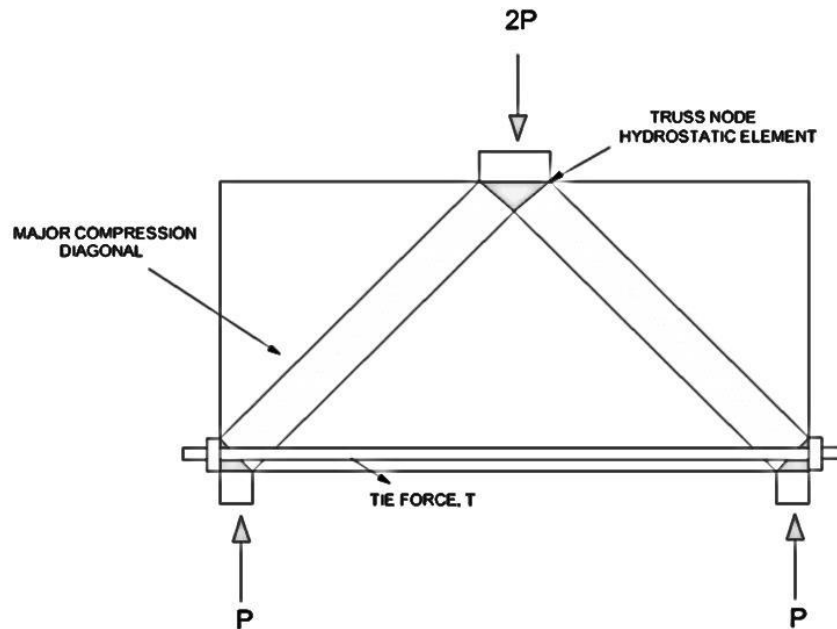


Figure 2.4: Arch action mechanism. Figure illustrating Compression diagonal struts, Tension ties and truss nodes

In this case, the lever arm ($j \times d$) does not remain constant over the length which implies there is no horizontal shear flow across the section and it may be because of the steel is unbonded or the shear flow is disrupted by an inclined crack extending from the load to reactions.

2.2.3 Model for Flexure-Shear Interaction

When beam develops a flexure shear interaction, the shear resistance consists of two different mechanisms, beam and arch mechanisms as shown in Figure (2.5) governed by the following equation.

$$\frac{a}{d} = \frac{m}{V * d}$$

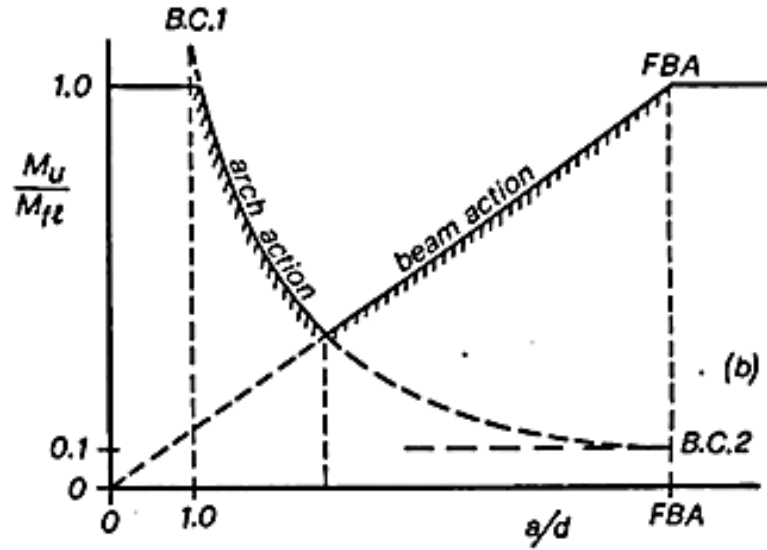


Figure 2.5: Flexure Shear Interaction

2.3 Primary Mechanisms of Shear Resistance

The primary mechanisms of shear resistance has been explained by rigorous analytical and experimental research. This mechanism includes three forces provided by concrete in compression zone, aggregate interlock and the dowel action across the longitudinal steel reinforcements. Any shear force, which exceeds or is surplus of the above three forces is resisted by shear reinforcement. The stirrups are generally placed vertically and anchored in compression zone to avoid slipping. In a cracked reinforced concrete beam with shear reinforcement, the shear is carried by the vertical component of shear force in compression zone concrete (V_{cy}), vertical component of aggregate interlock force at the cracked surface (V_{ay}), the dowel action of longitudinal reinforcement (V_d) and the force in the vertical stirrups (V_s). Internal distribution of the forces is shown in Fig 2.6.

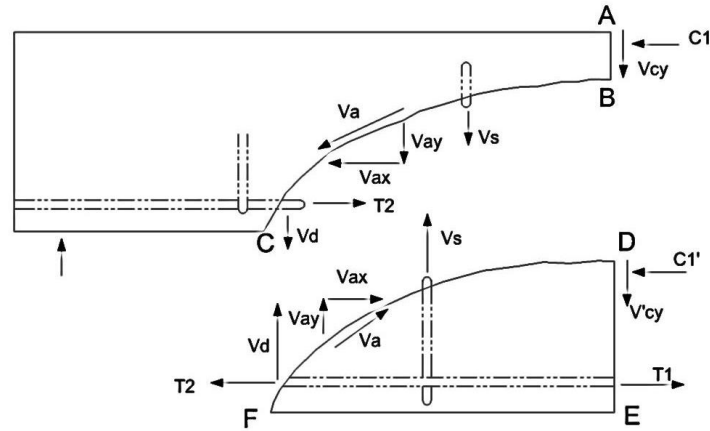


Figure 2.6: Internal forces developed across an inclined crack

2.4 Classification of Beams

The beams can be classified according to their shear span to depth ratio as:

1. Deep beams with $0 < a/d < 1$
2. Short beams with $1 < a/d < 2.5$
3. Normal beams (Slender Beams) with $2.5 < a/d < 6$
4. Very Slender Beams ($a/d > 6$)

2.5 Prediction of Shear behavior

When the principle tensile stress exceeds the tensile strength of concrete, it cracks. Moreover, cracks will be normal to the principle stresses. The principle stress direction coincides with the longitudinal axis of the member and hence cracks will be perpendicular to that direction (vertical). However, when the beam is subjected to both moments and shears the inclination of crack does not remain 45° but would depend upon several factors including the ratio of shear to moment, beam dimensions, presence of various types of reinforcement and the loading pattern. The principal stress trajectory is depicted in Figure (2.7).

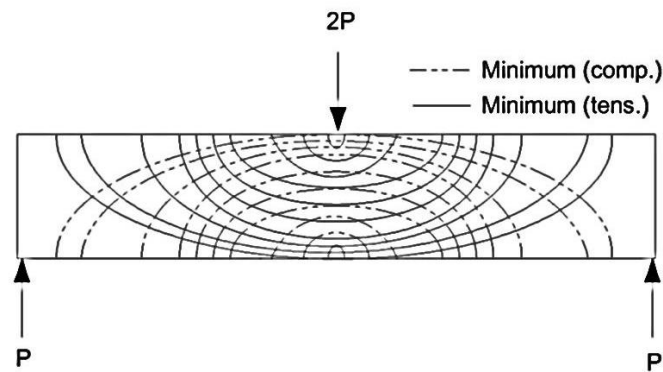


Figure 2.7: Principle Stress Trajectory

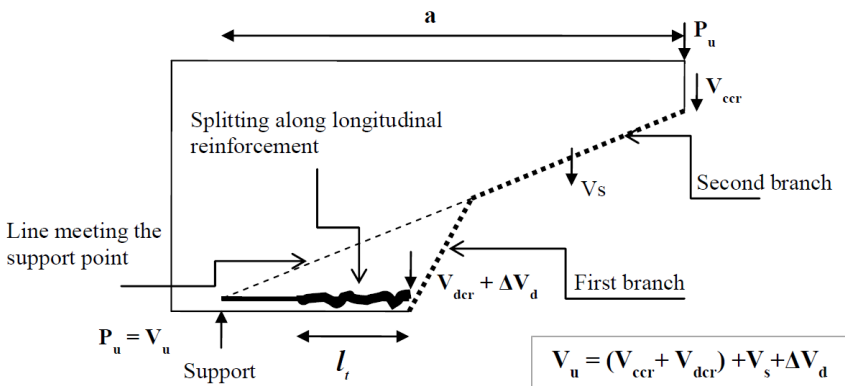
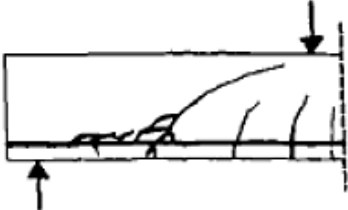
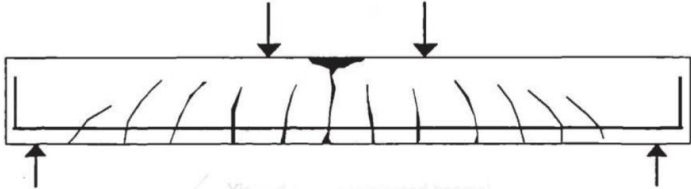
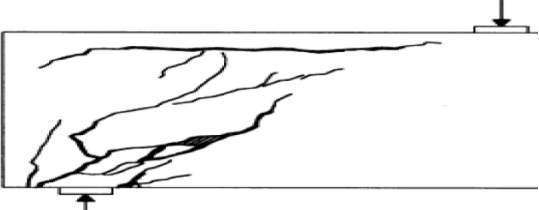
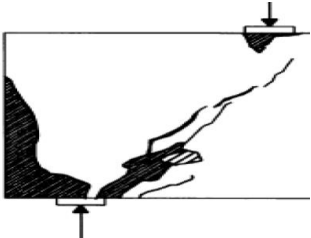
The similarity between the plane of maximum principal tensile stress and the initial cracking pattern can make one think it as a measure of gauging shear failure. However, this assumption of predicting crack initiation does not hold any significance as in normal RC structures, as the flexure cracks generally occurs before principal tensile stresses at the mid height becomes critical. Once, the flexure crack are formed, the tensile stress perpendicular to the crack drops to zero. To maintain equilibrium a major redistribution of stresses is necessary. Hence, we cannot predict the onset of inclined cracking from principle tensile stress unless shear cracking precedes flexural cracking.

2.6 Failure Modes in Shear

Following Modes of failure in beams have been identified in Literature Ziara (1993):

- Diagonal Tension Failure
- Shear Tension Failure
- Shear Compression Failure
- Flexural Failure
- Anchorage Failure
- Bearing Failure

Table 2.1: Failure Modes in Shear

TYPE OF FAILURE	FIGURE
<p>Diagonal Tension Failure (A)</p>	 <p>Diagram illustrating Diagonal Tension Failure (A). The beam is supported at the left end and has a load P_u at the right end. The shear force is V_u. The failure is characterized by a diagonal crack that splits along the longitudinal reinforcement. The diagram shows the first branch of the crack with shear force $V_{dcr} + \Delta V_d$ and the second branch with shear force V_s. The ultimate shear force is $V_u = (V_{ccr} + V_{dcr}) + V_s + \Delta V_d$. The length of the beam is a, and the length of the first branch is l_t. A line meeting the support point is also indicated.</p>
<p>Shear Tension failure (B)</p>	 <p>Diagram illustrating Shear Tension failure (B). The beam is supported at the left end and has a load at the right end. The failure is characterized by a diagonal crack that is perpendicular to the longitudinal axis.</p>
<p>Shear Compression Failure (C)</p>	 <p>Diagram illustrating Shear Compression Failure (C). The beam is supported at the left end and has a load at the right end. The failure is characterized by a diagonal crack that is parallel to the longitudinal axis.</p>
<p>Flexure Failure (D)</p>	 <p>Diagram illustrating Flexure Failure (D). The beam is supported at both ends and has a load at the center. The failure is characterized by a vertical crack at the center of the beam.</p>
<p>Anchorage Failure (E)</p>	 <p>Diagram illustrating Anchorage Failure (E). The beam is supported at the left end and has a load at the right end. The failure is characterized by a diagonal crack that is parallel to the longitudinal axis, indicating failure of the reinforcement anchorage.</p>
<p>Bearing Failure (F)</p>	 <p>Diagram illustrating Bearing Failure (F). The beam is supported at the left end and has a load at the right end. The failure is characterized by a diagonal crack that is parallel to the longitudinal axis, indicating failure of the concrete bearing capacity.</p>

2.6.1 Diagonal Tension Failure

The diagonal crack originates from the previous flexural crack developed. In case of slender beams (a/d between 2.5 and 6), failure occurs within the shear span. The crack propagates through the beam and reaches the compression zone and at critical loading, it is likely to fail as a consequence of concrete splitting there which is expected to happen suddenly in a brittle manner as shown in Table 2.1 (A). Ziara (1993)

2.6.2 Shear Tension Failure

The difference between diagonal tension failure and this type is that it applies to short beams. In this case too, the shear crack propagates through the beam but is not likely to cause the failure at its own. Loss of bond between concrete and longitudinal steel can also cause failure due to splitting cracks developing in this region. On reaching a critical loading point, beam fails as a consequence of splitting of the compression concrete as demonstrated in Table 2.1 (B). Ziara (1993)

2.6.3 Shear Compression Failure

Contrary to shear tension failure, if splitting cracks do not appear and the failure is caused merely due to diagonal shear crack propagating through the beam, it is termed as a *shear compression failure*. This mechanism is applicable on deep beams. In short beams, due to presence of arch action, the ultimate load causing failure can be much larger. See Table 2.1 (C). Ziara (1993)

2.6.4 Flexural Failure

Moment is basically responsible for initiation and propagation of flexural cracks which occur in slender beams. At the location where moment in the beam has the largest magnitude the appearance of cracks is more likely as demonstrated in Table 2.1 (D). Cracks develop when the concrete's shear stress reaches its tensile strength. Flexural cracks are nearly vertical and cause failure in the beam either due to excessive yielding of longitudinal

reinforcement in case of under reinforced beams, which may cause failure of concrete in tensile zone or due to concrete's crushing in compression zone before longitudinal reinforcement yields. Ziara (1993)

2.6.5 Anchorage Failure

Anchorage failure may be described as a slip or loss of bond of the longitudinal reinforcement (see Table 2.1 (E)). Dowel action can be linked to it where the splitting of concrete occurs as a consequence of failure of aggregate interlocking resistance around the bar.

2.6.6 Bearing Failure

The support fails when the bearing stresses surpass the bearing capacity of the concrete. This type of failure is referred to as *Bearing Failure*. The concrete at the support usually fails if the bearing plate is undersize, as shown in Table 2.1 (E).

2.7 Parameters influencing shear strength

Over the years, rigorous research and extensive experimental studies have tried to understand and predict the shear strength of reinforced concrete beams. Following are the list of all the parameters known to affect shear are:-

Table 2.2: Factors affecting Shear Strength

Parameter	Relation to shear	
Shear Span to Depth Ratio (a/d)	Change of shear transfer mechanism. (Leonhardt, Walther et al. 1964) Reason: The moment arm (jd) does not remain constant as the a/d decreases below 2.5 (deep beams)	
Depth of Members or Size Effect	Decrease in shear strength with the increase in effective depth (Shioya, Hasegawa et al. 1985) Reason: Increased width of diagonal cracks	
Axial Force	Dependent on axial force particularly for members without transverse reinforcement. Axial Tension: Shear strength decreases Axial Compression (applied load or pre-stressing): Shear strength increases Reason: Confining effect	
Longitudinal Reinforcement	Amount of minimum shear reinforcement ρ_v	Longitudinal Reinforcement ρ_l
	Increases	Decreases
	Decreases	Increases
	Reason: Balance of ρ_v and ρ_l required for achieving reserve strength and deflection	
Concrete Compressive Strength	<u>Component of Shear resistance provided by concrete</u> NSC: Aggregate interlocking component enhanced (irregular cracks due to difference in crushing strength of concrete and aggregate) HSC: minimal contribution because of aggregate interlocking affect.	

2.7.1 Shear Span-to-Depth Ratio (a/d)

The shear span-to-depth ratio (a/d) has a pronounced effect on inclined cracking and ultimate shears in case (a/d) is less than 2. Such shear spans are referred to as *deep (D) regions*. In case where (a/d) is greater than 2, Beam action mechanism dominates, and shear span-to-depth ratio has little effect on the inclined cracking shear.

2.7.2 Depth of Members or Size Effect

With increasing beam depth, the crack spacing and the crack widths tend to increase, this hampers the concrete's capability to transfer shear by aggregate interlocking mechanism.

An increase in the overall depth of a beam with very little or no web reinforcement results in a decrease in the shear at failure for a given shear span-to-depth ratio Collins and Kuchma (1999). However, in beams with at least the minimum required web reinforcement, the stirrups holds the crack faces together so that the shear transfer across the cracks by aggregate interlock is not lost. As a result, the reduction in shear strength due to size shown in is not observed in beams with web reinforcement.

2.7.3 Axial Force

Axial compressive force increases the load at which the incline cracking occurs, as the force is increased, flexural cracking phenomenon is delayed and the flexural cracks do not spread as far into the beam however axial tension has the opposite effect and decreases the inclined cracking load at failure. It directly increase the tension stress, and hence the strain, in the longitudinal reinforcement.

2.7.4 Concrete Tensile Strength

The inclined cracking load is a function of the tensile strength of the concrete. The stress state in the beam involves biaxial principal tension and compression stresses. When the tensile stresses on the beam exceed the tensile strength, tensile cracks formation occurs. Zararis and Papadakis (2001) discusses this phenomena in great detail where he analyzed the second branch of the critical crack leading to failure, he argued this failure is due to tensile splitting of concrete. The formula for ultimate shear failure for beams without web reinforcement is given by:

$$v_{cr} = \left(1.2 - 0.2 \frac{a}{d}\right) \frac{c}{d} f_{ct}$$

Where f_{ct} is the tensile splitting strength of concrete.

Some other factors affecting Shear strength are:-

- Load conditions
- Cross section shape
- Distribution of longitudinal reinforcement

2.8 Shear Theories

2.8.1 Shear Stresses in Un-cracked Beams

The shear stresses, v , on elements of a beam section can be calculated by traditional theory for homogenous, elastic, un-cracked beams as:-

$$v = \frac{VQ}{Ib}$$

Where,

V = Shear force on a cross section

Q = First moment about the neutral axis

I = Second moment of area of cross section

b = Width of member where stresses are being calculated.

It should be noticed that equal shearing stresses exist on both the horizontal and vertical planes through an element. The horizontal shear stresses are of importance in the design of construction joints, web-to-flange joints, or regions adjacent to the holes in beams. For an un-cracked rectangular beam, the above equation gives the distribution of shear stresses. See figure (2.8)

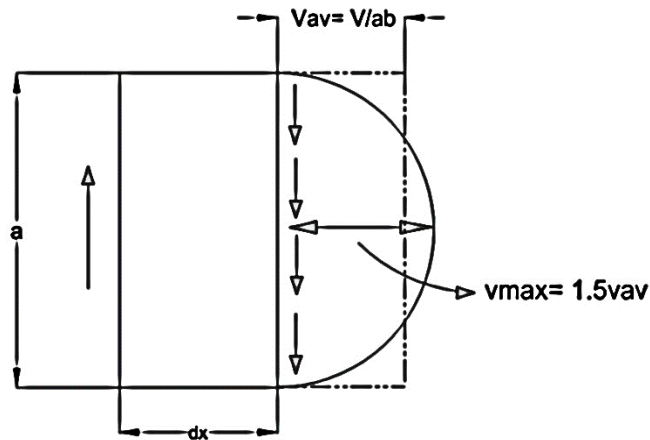


Figure 2.8: Distribution of Shear Stresses for un-cracked rectangular beam

This equation is an idealization of shearing stresses across a concrete section. However in reality this does not hold true as:

- Concrete is a heterogeneous material. It does not possess a constant modulus of elasticity.
- Concrete is subjected to creep therefore, it is not elastic.
- A section may be cracked and un-cracked and its determination is unpredictable, so that makes the computation of second moment of area and Young's Modulus far from being rigorously determined.
- Cracking causes the effective cross section of concrete to be variable along the length.

2.8.2 Comb Model by Kani

Kani (1964) put forward a comb model for idealizing the load carrying mechanism of RC beams cracked in flexure and subjected to shear. In this model the un-cracked concrete is represented by the back bone of the comb and concrete between flexural cracks is represented by teeth of the comb.

When the bending moment in a cantilever tooth becomes large enough to “break off” the tooth at its base diagonal cracking is considered to have occurred. Backbone thus serves as a tied arch.

Kani’s analogy can help us understand several aspects of the shear behavior of members without web reinforcement. This analogy also emphasizes the importance of bond on the shear transfer mechanisms. Kani’s model assumes that no shear stresses are transmitted across the flexural cracks. Later on several researchers found that even quite close to failure, the compression zone carried only 15% of the total shear and the remainder is carried by dowel forces in the flexural reinforcement and aggregate interlocking across the flexure cracks.

2.9 ACI Prediction of Minimum Shear Reinforcement

To avoid abrupt shear failure, ACI 318 – 11 specifies that minimum amount of shear reinforcement must be there in reinforced concrete beams. This minimum amount of transverse steel is intended to restrain the growth of diagonal cracks to avoid abrupt shear failure. Basing on previous experimental data for beams of normal and high strength concrete, ACI equation for minimum shear reinforcement has been developed. This equation is believed to have little consideration for the effects of longitudinal reinforcement and shear span to depth ratio. When minimum amount of shear reinforcement is provided in the beams, it holds the two cracked faces together, thus preventing the loss of shear transfer by aggregate interlock. Where required, the minimum shear reinforcement shall be computed by the equations (ACI Section 11.4.6.3) reproduced below. Eq 2.4 is new in the code and was introduced in ACI 318-05 to account for the influence of compressive strength of concrete.

$$A_{v(\min)} = 0.75\sqrt{f'_c} \frac{b_w s}{f_{yt}}$$

But not less than,

$$\frac{50b_w s}{f_{yt}}$$

ACI code restricts the spacing between shear reinforcement to half of effective depth or 24 inches for non prestressed members. This condition ensures interception of potential diagonal crack by at least one vertical stirrup.

2.10 Zararis Theory of Critical Shear Crack

Zararis proposes a theory which determines an expression for ultimate shear capacity of reinforced concrete slender beams obtained by adding a stirrup contribution to the shear capacity of beams without transverse reinforcement; and a criterion that must be satisfied by the minimum amount of shear reinforcement to prevent a brittle failure and restrain the growth of diagonal cracking.

2.10.1 Shear Strength of Beams without Transverse Reinforcement

The critical crack formation in slender beams without transverse reinforcement comprises of two branches. The first branch usually extends diagonally till the height of flexure cracks however second branch originates from its tip and extends through the compression zone and ultimately meets the point of load. The second branch is the reason for failure. An expression for nominal shear stress at the diagonal tension cracking is

$$v_{cr} = V_{cr} / bd = (c / d) f_{ct}$$

as demonstrated in Table(2.1). To account for the size effect on tensile strength, a correction factor is introduced to the previous equation

$$v_{cr} = V_{cr} / bd = \left(1.2 - 0.2 \frac{a}{d} \right) \frac{c}{d} f_{ct} \quad (1)$$

Where the term in brackets should not be less than 0.65 (d in m) The Shear force V_{cr} and the shear stress v_{cr} in Eq. (1) represent the ultimate shear and the ultimate shear stress.

2.10.2 Shear Failure Mechanism in Beams with Transverse Reinforcement

The pattern of cracking in this case is similar to the beams without stirrups. It is observed that the effect of stirrups can be considered negligible up till the initiation of the second branch of the critical crack and only then stirrups come into action. As the crack (second branch) propagates it gradually opens. This is caused by concrete shear force V_{ccr} at the beginning of the second branch to balance the developed force V_s of stirrups. Furthermore, the opening of the second branch of critical crack causes an increase ΔV_d of the shear force of the longitudinal steel bars. The Shear force V_{cr} at the beginning of cracking of the second branch of the critical crack is equal to the sum ($V_d + V_{ccr}$). Summing forces in the vertical direction and its equilibrium condition yield the following equation

$$V_u = V_{cr} + V_s + \Delta V_d \quad (2)$$

Where,

V_u = Shear force at shear failure.

V_{cr} = Shear force at the beginning of cracking of the second branch.

V_s = Force of stirrups along the critical diagonal crack

V_d = Shear force of bars of main reinforcement

The force ΔV_d is due to the opening of the second branch of the critical crack, but its existence is only due to the inclusion of stirrups in the beams. This force appears to be a new factor, influencing the shear strength in addition to the other two conventional factors. The shear force V_d of longitudinal steel bars brings about a horizontal splitting of concrete cover along the longitudinal reinforcement. This splitting results in the loss of the shear force V_d and, consequently, the failure of beam. Preventing this splitting hinders the shear failure. Zararis after examination of various related equation in equilibrium, devised an expression for this force $\Delta V_d = 0.5 \rho_v f_{yv} b d$ Zararis also determined the force of stirrups.

$$V_s = 0.25 \frac{a}{d} \rho_v f_{yv} b d$$

These expressions along with Equation 1 when substituted into Equation 2, yields the final expression for V_u shear force at equilibrium, which is as follows:

$$V_u = \left[\left(1.2 - 0.2 \frac{a}{d} \right) \frac{c}{d} f_{ct} + \left(0.5 + 0.25 \frac{a}{d} \right) \rho_v f_{yv} \right] bd \quad (3)$$

2.10.3 Zararis's minimum Shear Reinforcement

Zararis gave an analytical expression for the relationship he postulated between the required amounts of shear reinforcement to the ratio of the longitudinal reinforcement. As discussed earlier, the opening of the horizontal splitting crack along the main reinforcement, which has as consequence a proportional opening of the critical diagonal crack, is directly related to the value of V_d which is related to the amount of main reinforcement. The shear stress τ_{sxy} of the longitudinal bars is related to axial stress σ_{sy} through the equation.

$$\tau_{sxy} = 0.4 \sigma_{sy} / \tan \phi$$

which when related to ΔV_d equates to:

$$\Delta V_d = A_s \Delta \tau_{sxy} = 0.4 A_s \Delta \sigma_{sy} / \tan \phi$$

ϕ = angle between the direction of the second branch (critical crack) and the vertical direction

Taking approximation of the following values as $\tan \phi \cong a/0.8d$ and $\Delta \sigma_{sy} \cong 0.9 f_{yv}$ the above equation can be expressed as:

$$\Delta V_d = 0.28 \frac{\rho / \rho_v}{a/d} \rho_v f_{yv} bd \quad (4)$$

This expression once substituted to Equation 2 takes the form:

$$V_y = V_{cr} + 0.25 \left(\frac{\rho / \rho_v}{a/d} + 0.9 \frac{a}{d} \right) \rho_v f_{yv} bd \quad (5)$$

Shear force ΔV_d resulting from Eq. (4) can be much higher than the corresponding force ΔV_d given by $\Delta V_d = 0.5\rho_v f_{yv} bd$. Namely, the force ΔV_d at stirrup yielding can be much larger than that needed for the horizontal splitting. a large ratio of the longitudinal reinforcement (or a large ratio ρ/ρ_v) brings about a quick and significant increase of the force ΔV_d , which in turn overcomes the resistance of stirrups and forces them into premature yielding; and splitting along the main reinforcement occurs in any case when the force ΔV_d has the value given by ΔV_d ; afterwards, the surplus of force ΔV_d (difference of the values given by Eq. (4) and $\Delta V_d = 0.5\rho_v f_{yv} bd$) causes an extensive and wide opening of the splitting crack and, consequently, a significant opening of the critical diagonal crack. According to the above analysis, to avoid an undesirable widening of critical diagonal crack (as well as that of the horizontal splitting crack), a surplus of the force ΔV_d must not exist. This occurs when the value of ΔV_d given by Eq. (4) equals the one given by,

$$\Delta V_d = 0.5\rho_v f_{yv} bd \quad (6)$$

Equating these two equations

$$\rho/\rho_v \leq 1.75(a/d)$$

According to this ratio the stirrup yielding comes first and splitting of concrete cover occurs afterwards. But when the ratio $\rho/\rho_v > 1.75(a/d)$, the shear failure of a beam is accompanied by a quick and extensive splitting crack along the reinforcement, as well as by a significant widening of the critical crack.

2.10.4 Experimental Verification

With 20 sets of test data, 174 test results with various strengths of concrete (high and low), geometrical sizes, shear reinforcement ratios, shear span-depth (a/d) ratios, and longitudinal steel ratios have been obtained on slender beams. The test data list includes the test results of Leonhardt and Walther (1962); Bresler and Scordelis (1963); Placas and Regan (1971); Swamy and Andriopoulos (1974); Mphonde and Frantz (1985), Elzanaty, Nilson et al. (1986); (Johnson and Ramirez 1989), Anderson and Ramirez (1989), (Roller

and Russel 1990), Ahamad, Xie et al. (1994), (Yoon, Cook et al. 1996), Kong and Rangan (1998), Zararis and Papadakis (2001), Collins and Kuchma (1999) and Angelakos, Bentz et al. (2001)

Table 2.3: Comparisons of experimental and theoretical results of 174 beams performed by the above mentioned researchers

	ACI 318	Eurocode	Zararis Theory
	V_{exp} / V_{ACI}	V_{exp} / V_{EC}	V_{exp} / V_{theory}
Mean	1.252	1.092	1.004
COV %	16.78	18.26	10.23

*COV = Coefficient of Variation

2.11 Shear behavior of Normal Strength Concrete Slender Beams

Kashif Shehzad (2014) study of shear behavior of slender beams of normal strength concrete is an extension to the theory proposed by Zararis (2003). Kashif carried out an experimental study in order to analyze and validate the theory proposed by Zararis. His study incorporated all factor that contribute towards shear failiure incuding a new parameter development length (l_d)which was also incorporated. Taking into account all the factors, Kashif proposed a modified equation for minimum shear reinforcment provision, which is claimed to more accurate in determining the adequate amount of shear reinforcement. The proposed amount of shear reinforcemnet also leads to the development of nomial flexure capacity in RC beams. The experimental study based on the review has been devised. Eight full scale beams having moderate longitudinal reinforcement were cast and tested at shear span to depth ratio of 2.5. These samples are described as follows:-

Table 2.4: Kashif (2014) experimental program

Experimental Program	No. of Beams Tested
Beams without shear reinforcement	2
Beams with ACI minimum shear reinforcement	2
Beams with minimum amount of shear reinforcement as specified by P.D. Zararis	2
Beams with minimum amount of shear reinforcement estimated after incorporating changes in Zararis equation	2

2.12 Fracture Mechanics

In fracture mechanics, concrete is considered as a quasi-brittle material. When concrete is loaded close to its short term strength, inherent cracks start to extend slowly i.e., sub critically. These sub-critically growing cracks may reach a critical length for unstable, fast fracture propagation, resulting in a sudden failure of the specimen.

Following is the brief explanation of the available models.

2.13 Numerical Modeling of Concrete

2.13.1 Discrete Crack Approach

The crack is considered as a geometrical discontinuity. Crack is modelled, in an interface element that separates two elements, via displacement discontinuity.

Pros:

- Engineering problems exist whereby mechanisms of discrete cracks can be imagined to occur in a trend similar to yield line mechanisms. For that case the first 2 cons vanish and one may use the simple form of discrete cracks with predefined orientation.

Cons:

- It implies continuous change in node connectivity that doesn't fit in the basic attributes of finite element displacement method.
- Crack is constrained to follow a pre-defined path along element edge.

2.13.2 Smeared Crack Approach

A smeared crack concept visualizes the cracked solid to be a continuum and allows illustration in terms of stress strain relations. In diffuse crack patterns smeared cracks are

required for example large shear walls with densely distributed reinforcement.
Propagation is simulated by reduction of strength over the finite element.

Types

- Single (fixed crack orientation in the whole computational process)
- Fixed multidirectional (Intermediate of single fixed and rotating)
- Rotating crack model (rotating allows the orientation of crack with the rotation of principal axis)

Pros:

- Preserves the topology
- Doesn't impose restrictions with respect to orientation of the crack planes
- More realistic as considers the "bands of micro-crack" theory (but not much applicable)

Cons:

- Underlying assumption of displacement continuity conflicts with the realism of a discontinuity.

Standard fixed Smeared crack concept

- Mode 1 - Normal to the crack
- Mode 2 - Tangential to the crack
- Fixed Smeared crack concept with strain decomposition

2.13.3 Cohesive crack Model

Models the fracture process of quasi brittle materials. As the crack grows, it predicts the mechanical behavior of the specimen and crack path. A softening function $\sigma = f(w)$ is

the major constituent of cohesive crack model.

This function, a material property, relates the stress σ acting across the crack face to the corresponding crack opening width as shown in figure (2.9).

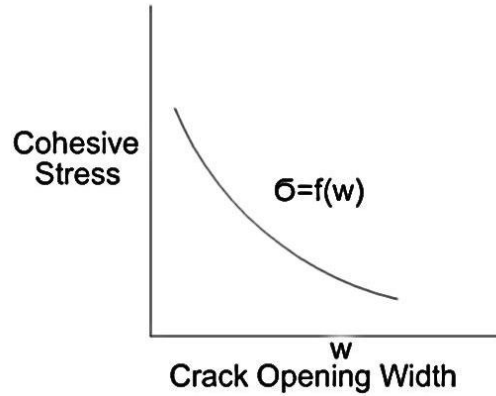


Figure 2.9: Relation between Cohesive Stress and Crack Opening Width

The summary of all the crack models is displayed in figure (2.10). (Hofstetter and Meschke 2011)

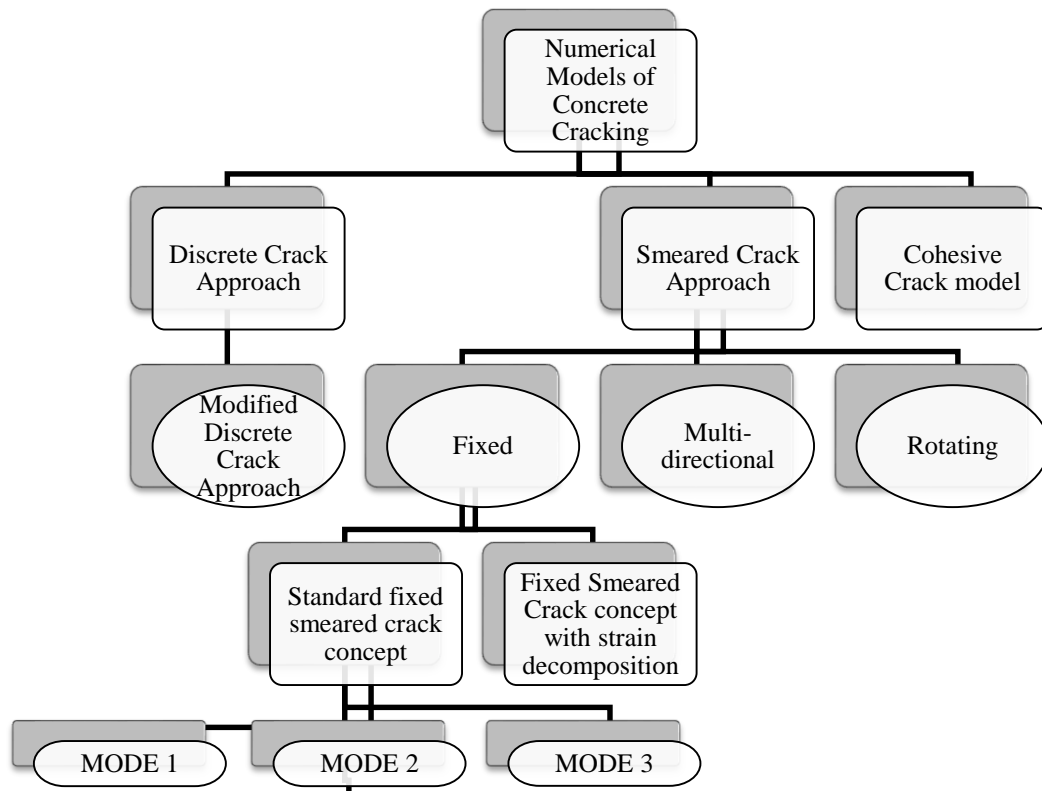


Figure 2.10: Hierarchy diagram of Concrete Cracking Model (Hofstetter and Meschke 2011)

RESEARCH METHODOLOGY

3.1 Methodology

The literature review focusing on available research on shear behavior of RC beams has been carried out. The behavior of 20 beams are studied in total. This research consists of benchmark and parametric analysis that have been explained separately below.

3.1.1 Benchmark Analysis

The benchmark analysis consisted of modelling 8 beams for calibration purpose. Models were prepared for different beams having varying amounts of shear reinforcement that were designed as per the minimum shear reinforcement given by ACI, Zararis, modified Zararis equation by Kashif and without shear reinforcement.

The results from finite element modelling were calibrated with the experimental values to validate the material parameters to be taken for the parametric analysis. The compressive strength of concrete and the amount of longitudinal reinforcement was kept same as of the experimental.

3.1.2 Parametric Analysis

After the model was calibrated, the research was extended further to varying shear spans to depth ratios. The depth however was kept constant, varying only the shear spans (by moving the loading point positions) to give a/d ratios ranging from 2.5 to 4. A total number of 12 beams were modelled to study the effects of shear span to depth ratio on beams with shear reinforcement.

After the analysis was done, the effect of shear span to depth ratio (a/d) was studied for beams. Later a comparison of predicted shear strength by ACI and modified Zararis equation is made with the experimental results and an equation, that is essentially a

modification in Zararis Equation for minimum amount of shear reinforcement to attain nominal flexure capacity, is presented at the end. These results have been systematically listed in the next chapter. The summary of the total number of beams and their corresponding parameters have been listed in the table below.

Table 3.1: Summary of the beams modelled in ABAQUS.

Beam No	f'_c (MPa)	b (mm)	d (mm)	$\frac{a}{d}$	Reinforcement		
					$\rho\%$	$\rho'\%$	$\rho_v\%$
Benchmark Analysis							
N1	27.6	254	406.4	2.5	1.482	0.385	0
N2	27.6	254	406.4	2.5	1.482	0.385	0
A1	27.6	254	406.4	2.5	1.482	0.385	0.131
A2	27.6	254	406.4	2.5	1.482	0.385	0.131
Z1	27.6	254	406.4	2.5	1.482	0.385	0.367
Z2	27.6	254	406.4	2.5	1.482	0.385	0.367
M1	27.6	254	406.4	2.5	1.482	0.385	0.275
M2	27.6	254	406.4	2.5	1.482	0.385	0.275
Parametric Analysis							
N3	27.6	254	406.4	3.0	1.482	0.385	0
A3	27.6	254	406.4	3.0	1.482	0.385	0.131
Z3	27.6	254	406.4	3.0	1.482	0.385	0.367
M3	27.6	254	406.4	3.0	1.482	0.385	0.275
N4	27.6	254	406.4	3.5	1.482	0.385	0
A4	27.6	254	406.4	3.5	1.482	0.385	0.131
Z4	27.6	254	406.4	3.5	1.482	0.385	0.367
M4	27.6	254	406.4	3.5	1.482	0.385	0.275
N5	27.6	254	406.4	4.0	1.482	0.385	0
A5	27.6	254	406.4	4.0	1.482	0.385	0.131
M5	27.6	254	406.4	4.0	1.482	0.385	0.275
Z5	27.6	254	406.4	4.0	1.482	0.385	0.367

While N Series refer to beams without shear reinforcement, A series refer to beams with minimum shear reinforcement specified by ACI code, while the Z and M refer to beams with minimum amount of shear reinforcement as proposed by Zararis and Kashif.

3.2 Simulation Specifications

The beams were modelled in commercial software called *ABAQUS® Version 6.13*. The following table represents the general settings chosen for this analysis.

Table 3.2: ABAQUS/Standard settings for the analysis

	ABAQUS/Standard	
Analysis type	Non-Linear Static Analysis	
Solution Technique	Stiffness-based solution technique based on increments (Newton-Raphson Method)	
Element Type	Finite Element	
Family	Concrete	Continuum/Solid
	Reinforcement	Wire/Truss
Order of Interpolation/ No of Nodes	Linear with hourglass control	
Integration Type	Reduced Integration	

3.3 Software Model

The spatial finite element model (FEM) of the rectangular cross section beams with transverse aligned stirrups and distributed longitudinal reinforcement is defined. The model is analyzed by nonlinear static analysis.

3.3.1 Beam Solid Model

The rectangular beam is modelled using solid 3D deformable body. The cross section is defined and then extruded to achieve three dimensional body shape. The deformable type is selected to include meshes and conduct smeared analysis. An 8-noded linear brick C3D8R, *reduced integration elements with inherent hourglass control* were assigned for the beam member.

3.3.2 Steel Truss model

The steel reinforcement bars are modelled as deformable wire/line truss elements. This type of element is chosen because of the type and geometry of the reinforcement bars. Truss element is assigned as steel reinforcement supports loading only along the axis or the centerline of the element. A 3-node linear 3D truss element (T3D3) for the rebar was assigned with linear geometric order. It uses quadratic interpolation for position and displacement so that strain varies linearly. Cross sectional area is defined corresponding to the truss element.

Embedded element

The steel reinforcement bar elements are defined as embedded elements. The embedded element technique is used to specify that element is embedded in host element. The geometric relationship between nodes of embedded and host elements is established. The translational degrees of freedom of the embedded nodes are eliminated and constrained to interpolated values of degrees of freedom of nodes of host element. Rotational degrees of freedom of the embedded nodes are not constrained. Three dimensional truss element in beam element type of embedded model is assigned to demonstrate reinforced beam model. Tolerance according to weight factors adjusts the nodes of embedded element to lie close to element face or edge to increase computational efficiency.

3.3.3 Displacement control deflection

A general static step using displacement control is defined in the model. The reference point/node is established at loading points and displacement control boundary conditions are applied at these points/node. The displacement was ramped linearly over the step time. Newton Raphson Method was employed for the mentioned analysis step and the conjugate loads (reaction force) were determined to generate the load vs. deflection curves. Newton Raphson Method utilizes quadratic convergence and gives accurate results. Few iterations are needed as adaptive tangent technique is adopted. The adaptive tangent technique is

applicable up to peak curve stress value. Hence large computational cost within one iteration is required.

3.3.4 Analytical rigid node/ surface

A rigid body is collection of nodes, elements or surfaces whose behavior and motion is governed by motion of single node called as rigid body reference node. Analytical rigid surface is used to define loading and supporting surfaces. This is done as analytical rigid surface does not need to be meshed and is described by analytical function. This helps to decrease the element number and hence the computational effort during analysis. The surfaces (not under scope of study), such as supports and loading plates, are modelled as rigid analytical surfaces so that computational effort is minimized.

3.3.5 Material Model

The reinforced beam was assigned material when defining the model. Both concrete for beam and steel for reinforcement were modelled. Different models are available in finite element software that portray material behavior and properties.

3.3.5.1 Steel

The steel is modelled according to the provided test results of stress strain curve. The density of the steel is mentioned in model. The elastic part of the stress strain curve of steel is modelled by inputting Young's Modulus and the Poisson's ratio. For the plastic part of stress strain curve the yielding stress and the corresponding plastic strains are entered in the model to define steel plasticity. The experimental stress strain curve is used to determine the mentioned parameters. In our case, the yield stress and plastic strain were fed in the form of x-y data extracted from the excel sheets provided by the Fazal Steel Mills, Industrial Area I-9 ,Islamabad.

3.3.5.2 Concrete

The concrete can be modelled in finite element model software by various provided models. The concrete is modelled in ABAQUS FEM software using concrete damaged plasticity model (CDP model). The concrete damaged plasticity model uses the concept of isotropic damaged elasticity along with isotropic compressive and tensile plasticity which represents the inelastic behavior of concrete. This model is usually used for reinforced concrete structures and is based on the smeared crack approach.

The linear elastic part of stress strain curve is modelled using the Young's Modulus of the concrete attained by ACI code formula. The strength of the concrete is 4000 psi as determined from cylindrical crushing tests performed in the laboratory. The plastic non-linear part of the stress strain curve is modelled both for the compressive and tensile part of the curve. The yield stress in compressive non-linear part of the stress strain curve is modelled along with its corresponding plastic strain. Similarly the yield stress in tensile non-linear/plastic part of curve is modelled with corresponding cracking strain.

The damaged states in tension and compression are represented by two hardening variables. The elastic plastic response of the concrete is described in terms of effective stress and hardening variables. Increased values of hardening variable indicate micro cracking and crushing in concrete model. Unloading concrete at any point on strain softening branch of the stress strain curve leads to the weakening of the unloading response as the elastic stiffness of concrete material is damaged or degraded. This is due to the plastic behavior of the concrete post the yielding point on stress strain curve. The degradation and damage is significantly different for both tension and compression tests but the degradation effect in stiffness is more pronounced when plastic strain increases. This degradation is characterized by two damage variables, for compression and tension, which are functions of plastic strains and other field variables. The uniaxial degradation variables are increasing functions of plastic strains ranging from zero, for the undamaged material, to one, for the fully damaged material.

The constitutive equations developed by Wang and Hsu were used to develop the post failure stress strain response of concrete for tension stiffening. Similarly to model the plastic response of the concrete in compression, Compressive Behavior was defined in concrete damaged plasticity model using the inelastic strain and yield stress calculated from the stress strain response generated calculated by using the constitutive equation provided by Carreira and Chu. Special focus was given to their applicability and limitations, for example the constitutive equation given by Carreira and Chu is only applicable to beams whose the f_c' is less than 5 ksi and is calculated experimentally by ASTM C39 which in our case was satisfied.

3.3.6 Concrete Material Input Properties

For concrete compressive behavior the following equations of Carreira and Chu (1985) were employed.

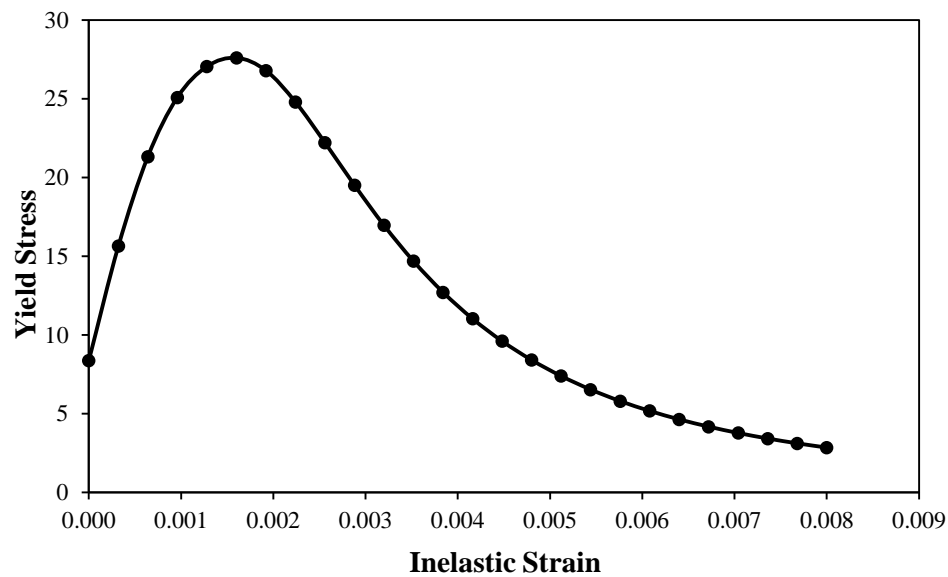


Fig.3.1: Concrete Compression Damage

$$\varepsilon'_c = (0.71f'_c + 168) \times 10^{-5} \qquad \beta = \left[\frac{f'_c}{32.4} \right] + 1.55$$

$$\frac{f_c}{f'_c} = \frac{\beta \left(\frac{\varepsilon}{\varepsilon'_c} \right)}{\beta - 1 + \left(\frac{\varepsilon}{\varepsilon'_c} \right)^\beta}$$

$$\beta = \left[\frac{f'_c}{4.7} \right]^3 + 1.55$$

For concrete tensile behavior the following equations of Wang and Hsu (1994) were employed

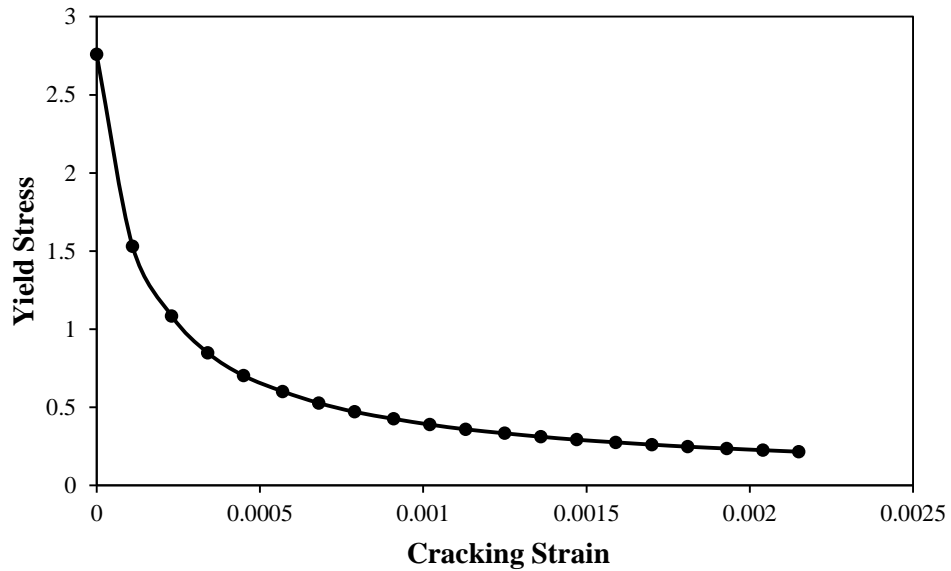


Fig.3.2: Concrete Tension Damage

$$\sigma_t = f_{cr} \left(\frac{\varepsilon_{cr}}{\varepsilon_t} \right)^{0.4} \quad f_{cr} = 4\sqrt{f'_c} \text{ (psi)}$$

$$\tilde{\varepsilon}_t^{ck} = \varepsilon_t - \varepsilon_{0t}^{el} \quad \varepsilon_{0t}^{el} = \frac{\sigma_t}{E_0}$$

3.3.6.1 Tension stiffening

Tension stiffening is the structural property of reinforced concrete that refers to the contribution of concrete between cracks in the overall stiffness of the member before the reinforcement yields. Concrete carries tension between cracks and the axial load is carried by the dowel action of the longitudinal reinforcement. The rigidity of the reinforced member or beam controls the deflection and crack initiation.

With the development of crack, the concrete loses its stiffness and concrete softening behavior initiates. Tensile stress in concrete decreases gradually and is counteracted by tension of the reinforcement bars. Stress variation in concrete near cracks reduces and increases in reinforcement in cracked region.

3.3.6.2 Bond slip

The bond slip occurs where the bond and interaction is developed between the concrete and the steel bars. It has three main components; chemical adhesion, mechanical interlock and friction. Chemical adhesion is the original bond developed between concrete and steel before any slip occurs. This bond breaks at certain loading after which it cannot provide adhesion. Relative movement between the steel and the concrete can now occur once the chemical bond is broken. Now the friction plays its part resisting the slip forces acting radially around the steel reinforcement.

As the concrete stress increases and reaches the peak value most models do not cater relationship past this peak value. The post peak tension stiffening of concrete due to progressive cracking is modelled in the model. The reduction in stresses post peak is determined and incorporated to determine reduced stresses in the concrete, which in other models is not applicable. Load interaction between the reinforcement and concrete in tensile zone is modelled as well. This reduction in post peak stresses is a resultant of bond slip developed due to friction and mechanical interlocking of concrete and steel reinforcement or within concrete itself and it increases with crack growth.

3.4 Simulation in ABAQUS (FEM software)

The simulation program comprised of modelling 20 beams in ABAQUS. By the use of boundary conditions for symmetry, only quarter beam was modelled. This ensured less computational time and allowed possibility of using finer mesh to achieve better represented contouring results in the model.

The beam is modelled using continuum (solid) elements .The truss elements are used to model the longitudinal and transverse reinforcement. The reinforcement is linked to adjacent concrete using the embedding technique. The effects of concrete steel interaction such as bond slip and dowel action are modelled using the tension stiffening.

Concrete damaged plasticity model has been employed to introduce damage inside the material. Following steps have been followed.

While working in FEM software, care must be ensured in keeping units consistent.

ABAQUS Standard suit is utilized for the modelling and simulation as it is a special purpose Finite Element analyzer that employs implicit integration to solve highly nonlinear systems with complex contacts and transient loads.

3.4.1 Parts definition

The ABAQUS FEM software presents module to create individual parts to be included in the model. The parts are created either in 2D or 3D according to model requirements. Deformable or rigid bodies can be created for the parts established. Parts can be given their base feature and shape such as solid (extrusion) or wire element.

3.4.2 Material definition

Different materials can be defined for the parts in the property module. Here general and mechanical (elastic and plastic) properties can be defined for various materials used in the model. Partitioning and establishment of reference points on parts can be made to facilitate assembly and post processing of model.

3.4.3 Section assignment

Sections are created in property module which contain information about the properties of the part or region. The section provides information about the region's cross sectional geometry. These sections are assigned to parts and regions which automatically gets assigned to all instances of the specified part.

3.4.4 Assembly/ Interaction

In the assembly module the orientation of different instances is developed and the mutual interactions (Interaction module) and constraints established. Boundary conditions are used to create supports and restrict movement along certain axis to guide model behavior.

3.4.5 Meshing

The parts are meshed using the structured meshing. The seeding size and then meshing is done in the module. The type of element for the part or surface can be specified here. Geometric order of the element to be analyzed is specified in this module as well.

3.4.6 Step formation

Steps are created in Step module where procedure type of the analysis is selected. Procedure types such as static general, dynamic implicit etc. are available to choose from. In the step the time period of the analysis and the incrementation during the time period is specified.

3.4.7 Loading/ Boundary Conditions

Loads and boundary conditions can be assigned in the Load module. Type of loading and its location is specified here, unless displacement control method is used. Displacement controls can be specified by displacement boundary condition in this module as well.

3.4.8 Field Output

Field History Output module selects different outputs parameters to be verified during analyzed. These output parameters are analyzed during the job running or the analysis. The job is created in the Job module in which different steps defined earlier are run to be analyzed.

3.4.9 Visualization

In the Visualization module, the analyzed job can be viewed and the output parameters of the analysis be achieved. The output data is retrieved in the module and different graphic and visual simulations show output results of the analysis. Graphs (XY Data), charts are also retrieved to evaluate relationship of different parameters.

MODELLING RESULTS

4.1 Choice of Mesh Size

The results are extracted in the post-processing module in ABAQUS that enables users to determine the desired output variables. As established before, the selection of element size and number is really important for any finite element modelling. An 8 noded hexahedral with hourglass control was selected as mentioned earlier. However for the number of elements that give a stable values of field output variables was determined through multiple number of analysis. Although the variables gets stable at elements more than 10,000, the element number was intentionally chosen as 29000 to get narrow crack bands and hence better visualization of cracking patterns.

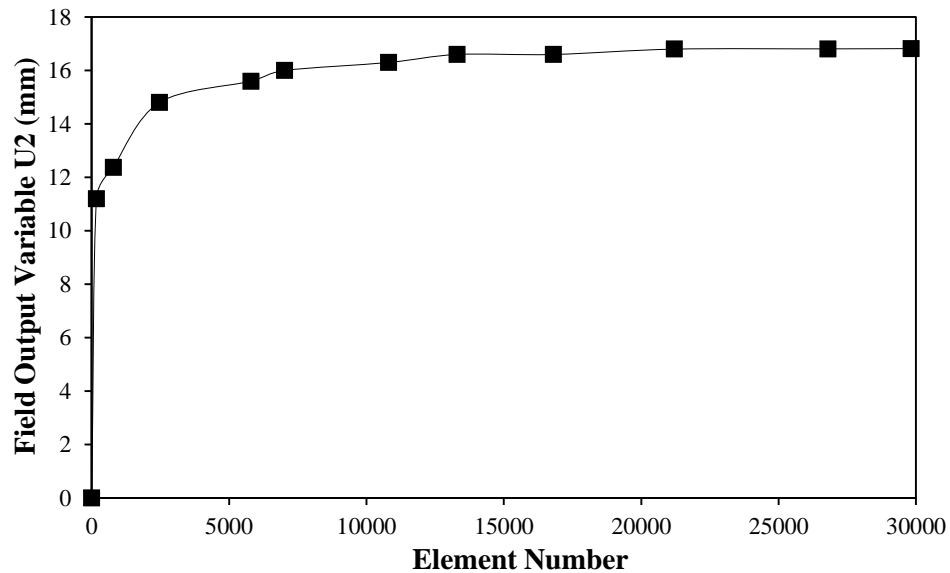


Fig-4.1: Stabilization of U2 with the increase in element number

4.2 Effect of dilation angle Ψ and Viscosity Coefficient ν for material calibration

The dilation angle primarily affects the plastic region of load-deflection behavior and results in the increase in load carrying capacity and displacement at failure. The converse is true for viscosity parameter where with the decrease the displacement at failure increase significantly. The analysis of the beams with varying dilation angle and viscosity parameter is shown in tabular form.

Table 4.1: Error with Dilation angle and Viscosity parameter variance

Varying Parameter		Percentage Error %
dilation angle Ψ	Viscosity coefficient ν	
25	0.01	33.2%
31	0.01	23.75%
35	0.01	15.24%
35	0.005	39.77%
38	0.01	17.85%
38	0.005	42.67%

The load-deflection curve corresponding to different values of dilation angle and viscosity parameter has been shown in the figure below:

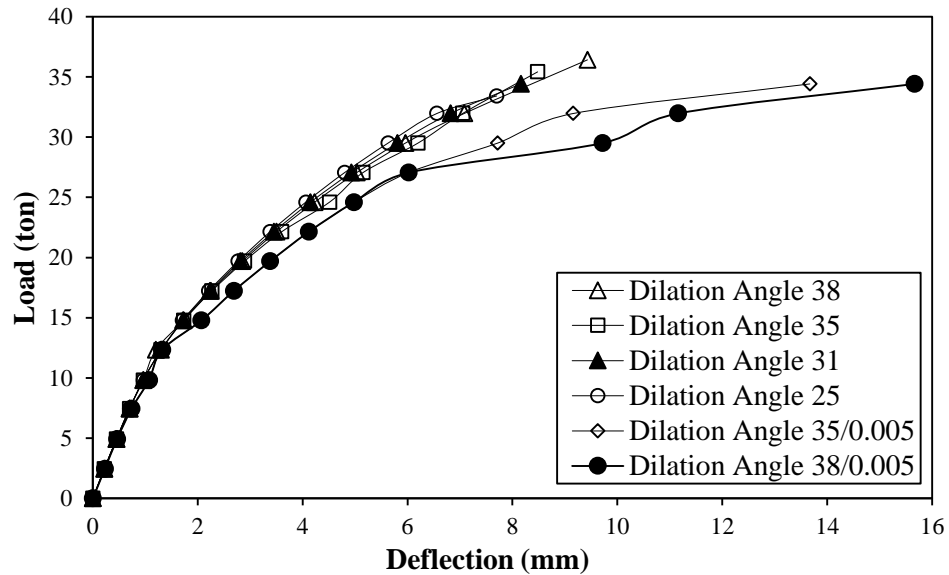


Fig 4.2: Effect of dilation angle and viscosity parameter on the load-displacement characteristics

4.3 Determination of Shear Strength (V_u) of the concrete beam for all sections

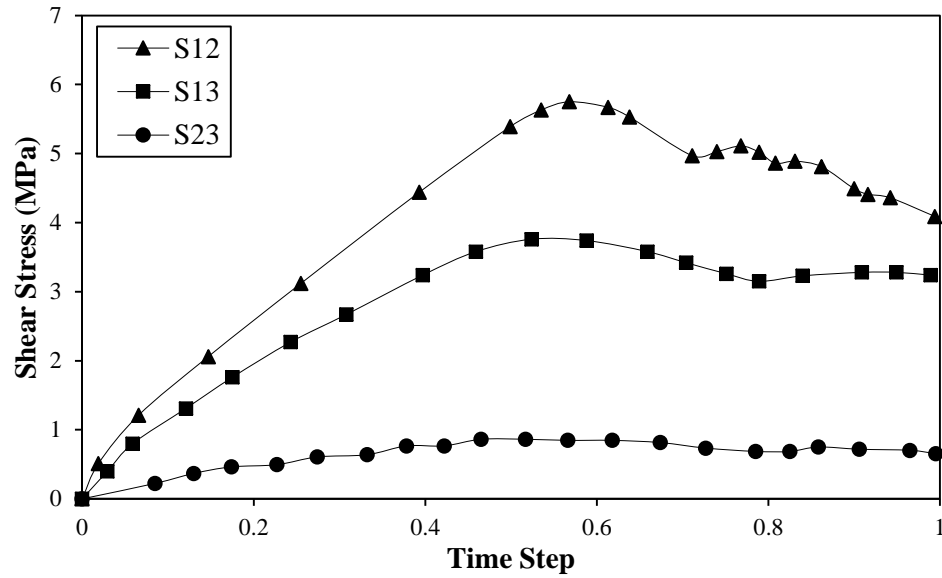


Fig 4.3: Shear Stresses along the three planes plotted verses step time

Where,

S12 corresponds to xy plane

S13 corresponds to xz plane

S23 corresponds to yz plane

The shearing stress along the three planes were determined and the nodes corresponding to the centroid of the material geometry were selected. The stress envelope corresponding to the all three axes was generated and the value of the shear strength for the whole material was taken as the minimum shear stress at while the material fails along any of the three axes is taken as the critical stress.

4.4 Load-Displacement characteristics of experimental versus the FEM results

The following figures show the Load-Deflection plots that were calibrated with the experimental results. The *xy* data has been attached separately in Appendix.

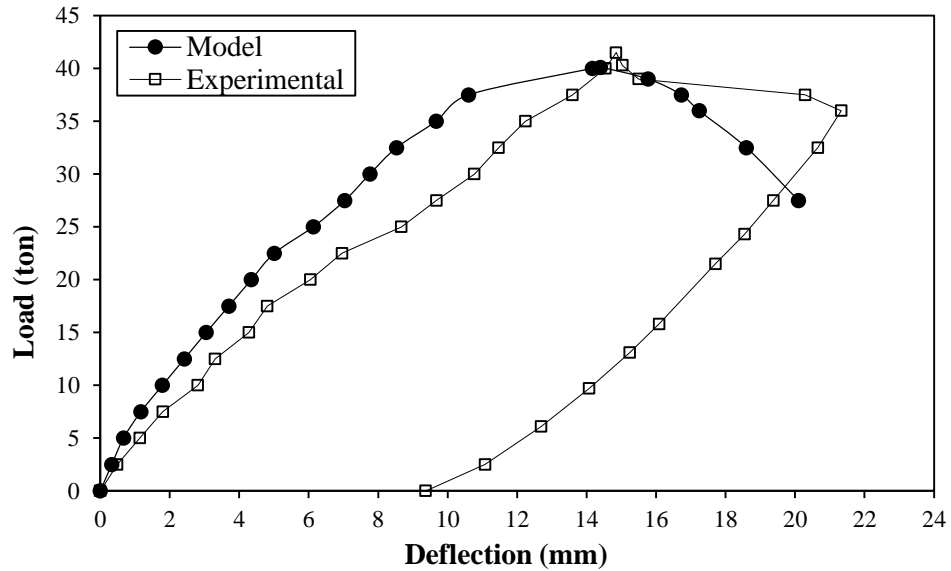


Figure 4.4: A1 Beam Load vs. Deflection at midpoint

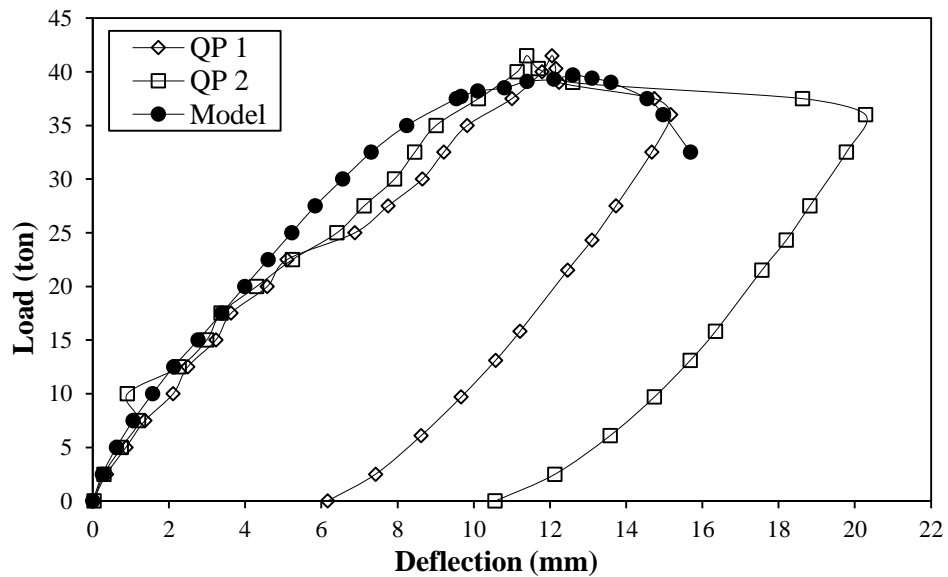


Figure 4.5: A1 Beam Load vs. Deflection at quarter points

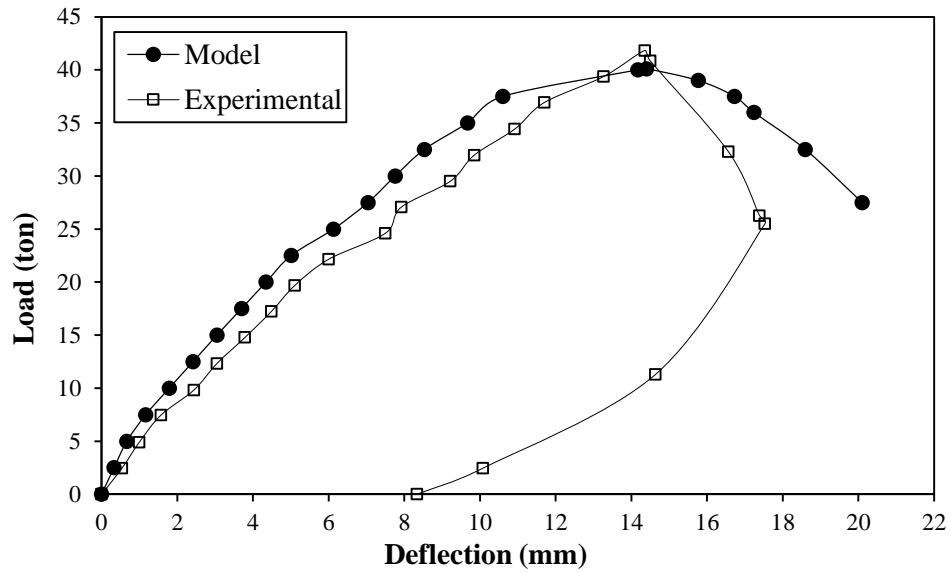


Figure 4.6: A2 Beam Load vs. Deflection at midpoint

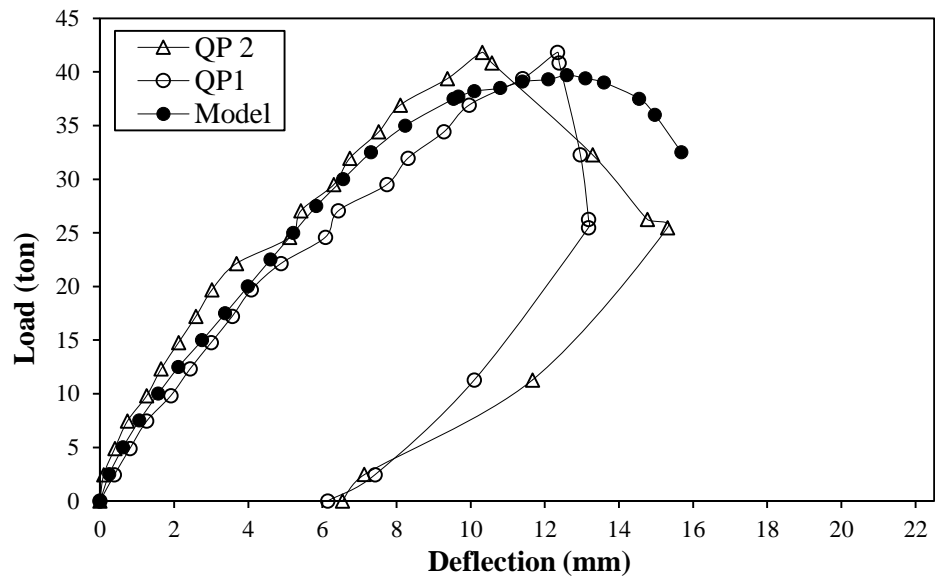


Figure 4.7: A2 Beam Load vs Deflection at quarter points

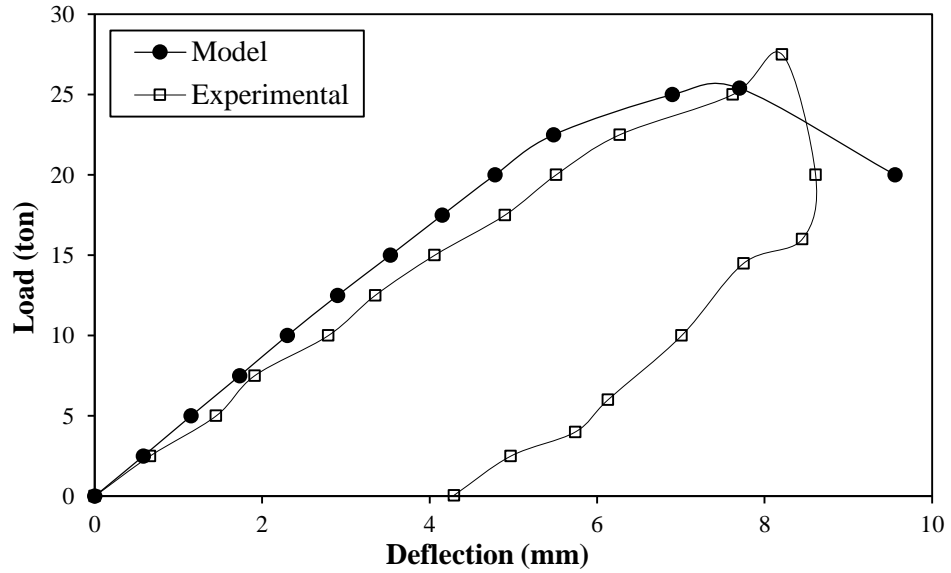


Figure 4.8: N1 Beam Load vs. Deflection at midpoint

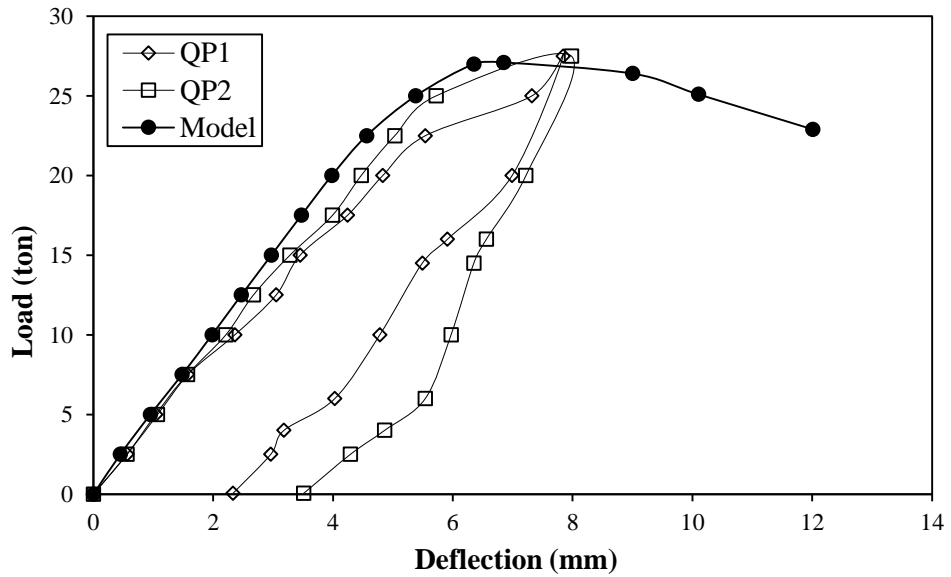


Figure 4.9: N1 Beam Load vs. Deflection at quarter points

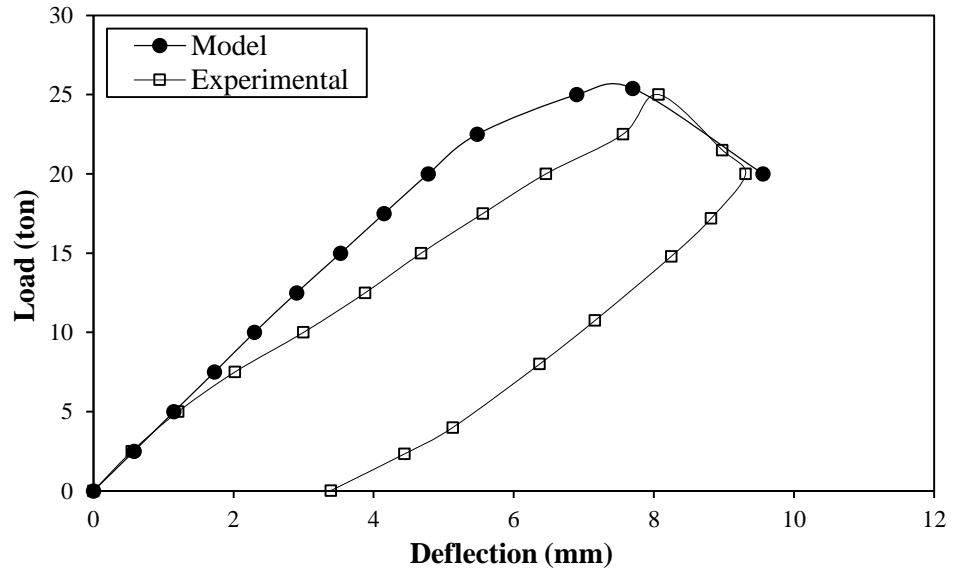


Figure 4.10: N2 Beam Load vs. deflection at midpoint

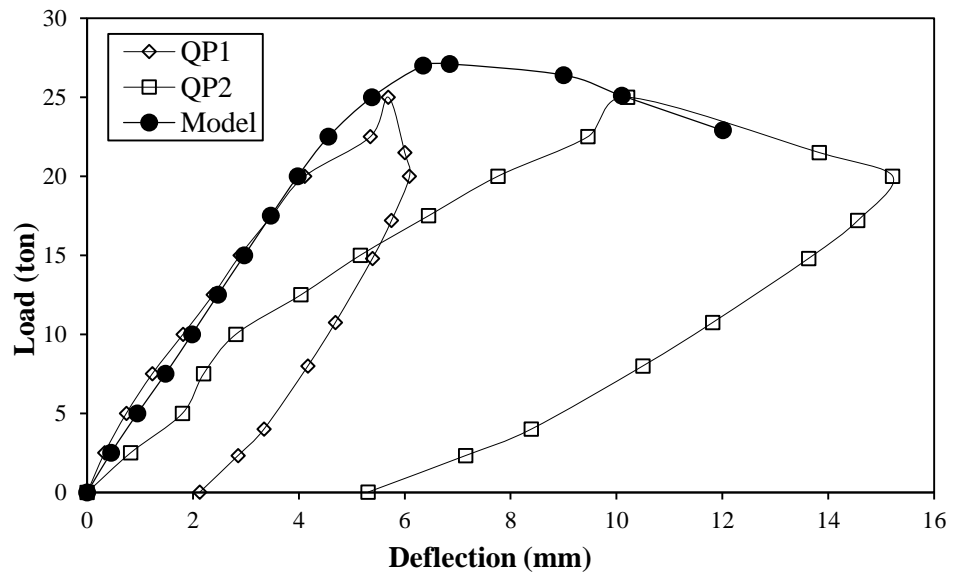


Figure 4.11: N2 Beam Load vs. deflection at quarter points

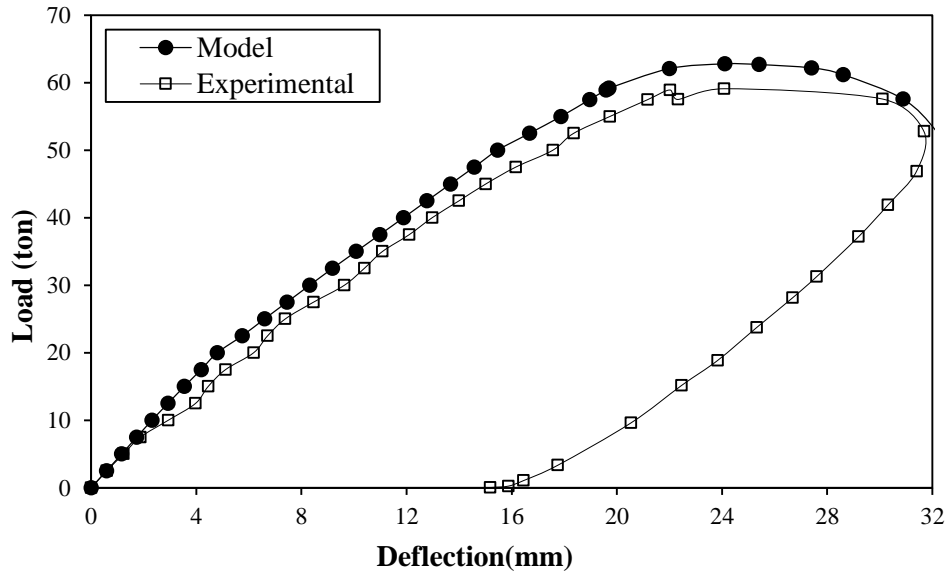


Figure 4.12: Z1 Beam Load vs. Displacement at midpoint

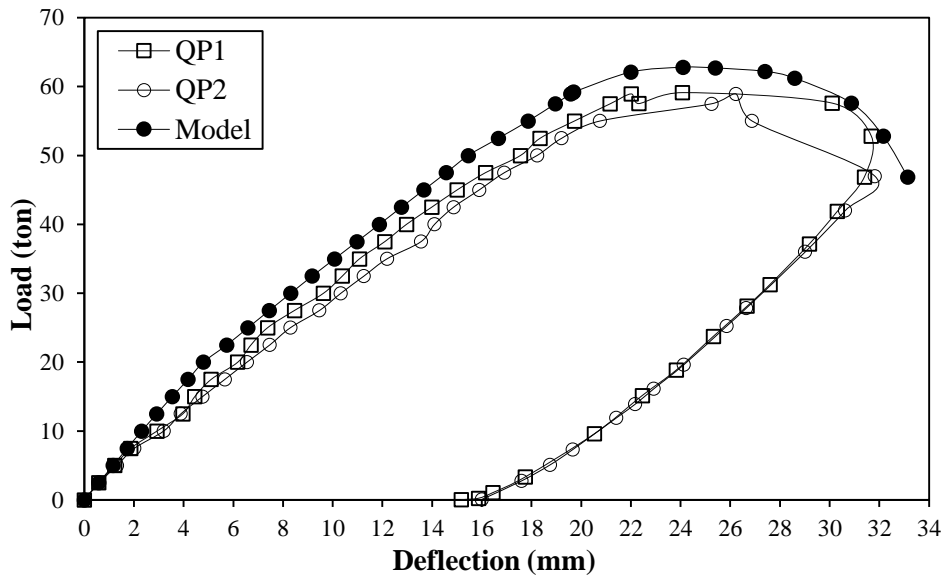


Figure 4.13: Z1 Beam Load vs. Deflection at quarter points

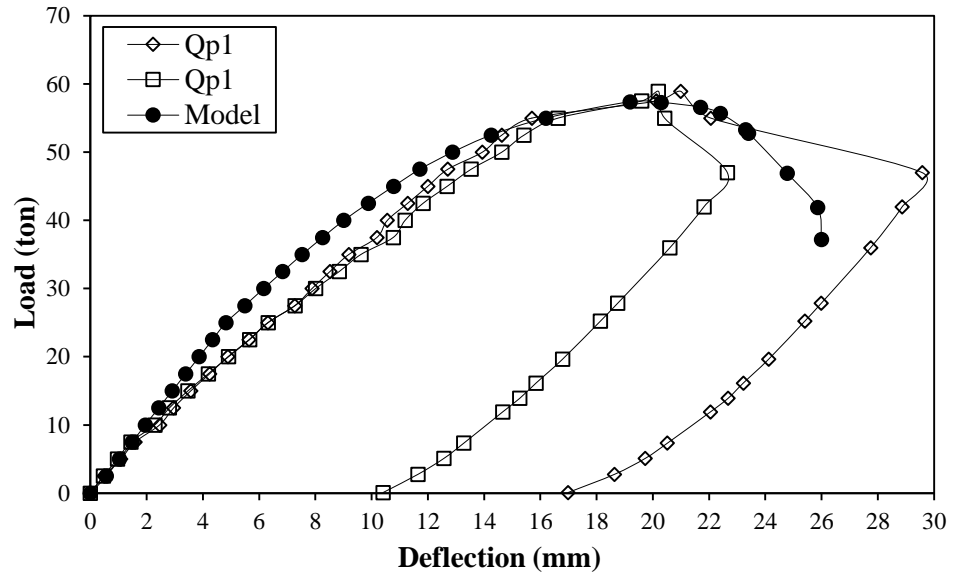


Figure 4.14: Z2 Beam Load vs. Deflection at quarter points

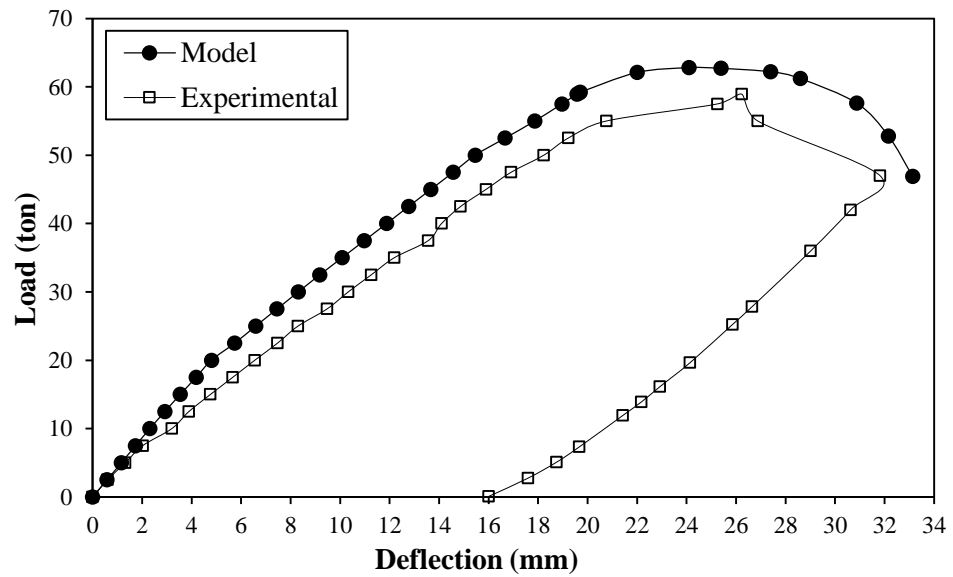


Figure 4.15: Z2 Beam Load vs. Deflection at midpoint

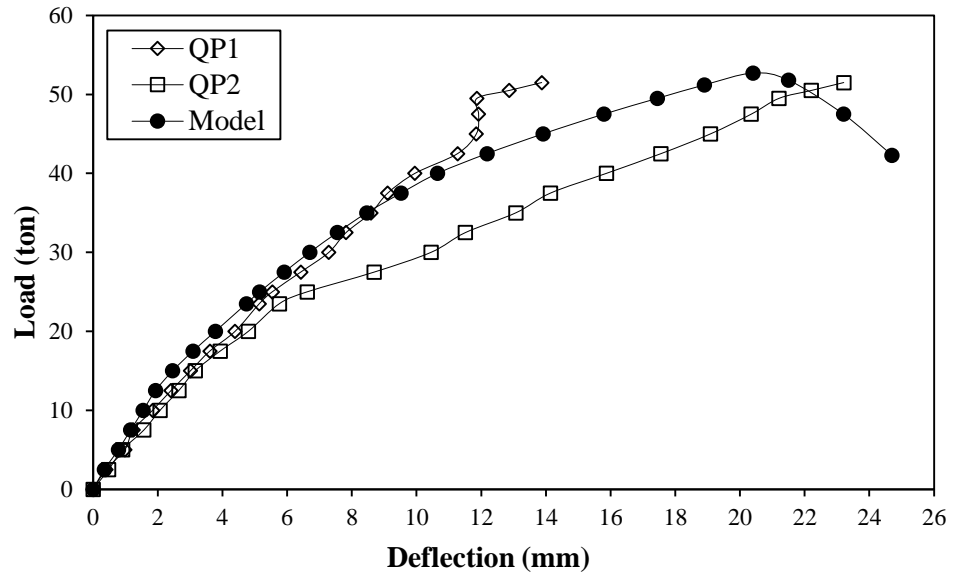


Figure 4.16: M1 Beam Load vs. Deflection at quarter points

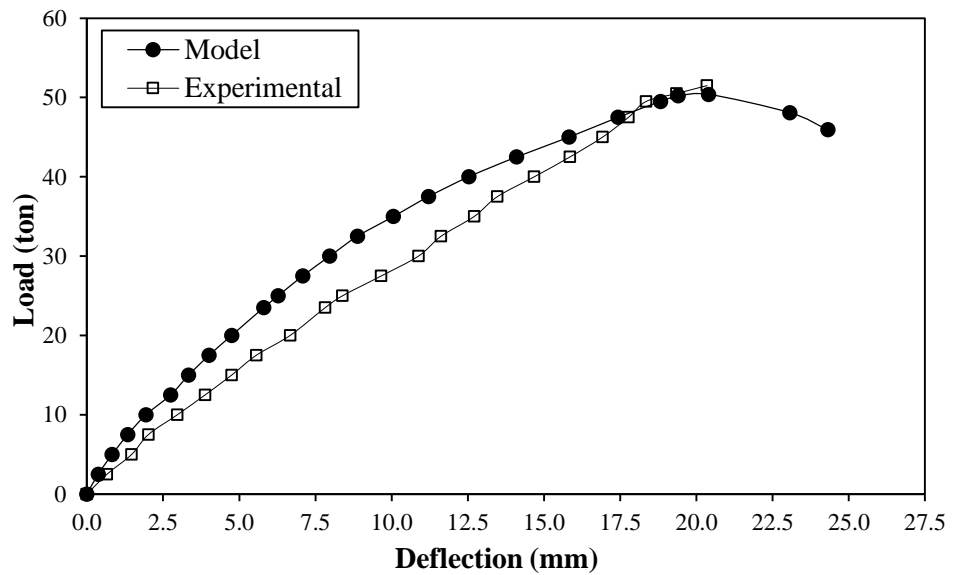


Figure 4.17: M1 Beam Load vs. Deflection at midpoint

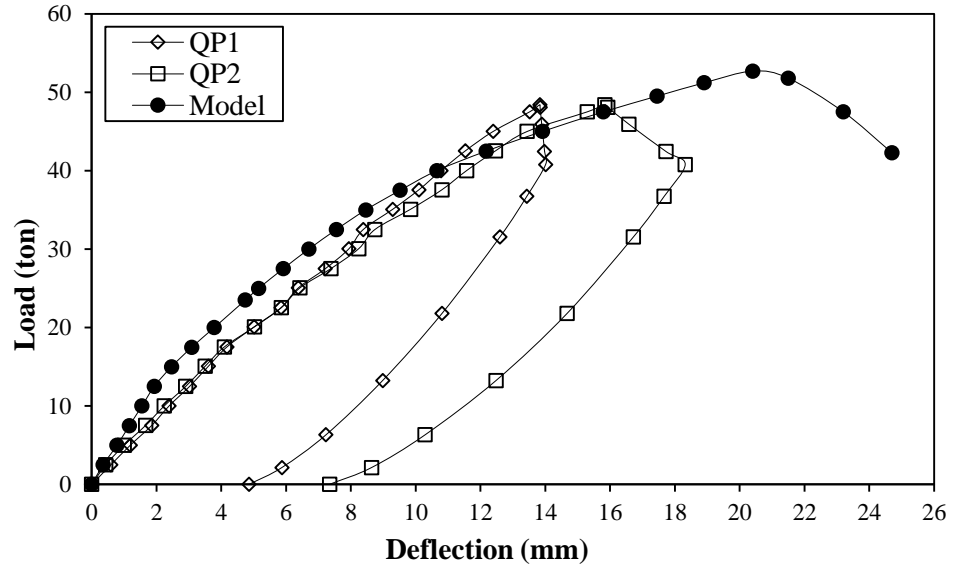


Figure 4.18: M2 Beam Load vs. Deflection at quarter points

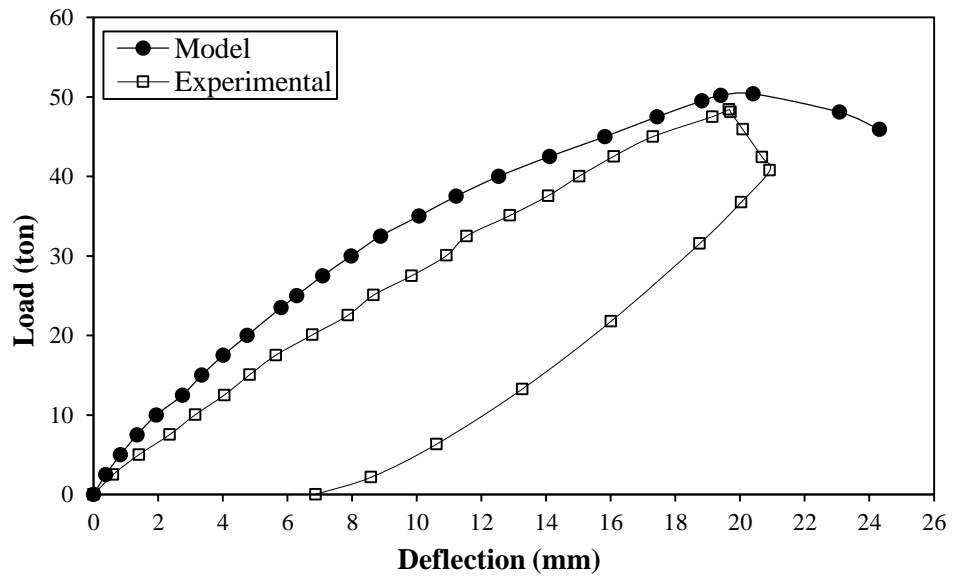


Figure 4.19: M2 Beam Load vs. Deflection at midpoint

CHAPTER 5

ANALYSIS AND INTERPRETATION OF RESULTS

After the results were extracted in the pre-processing module, the interpretation of results is made and the underlying trends have been discussed in depth in this chapter. The main aim of varying the amount of shear span was to analyze the effect of increasing shear span on the value of ultimate shear strength of the beam with constant depth. After the trend is studied a comparison between ACI predicted strength and that predicted by the Finite Element Model are tabulated in this chapter. The beams and their details are as follows:

Table 5.1: Specifications of N, A, Z and M series beams

Beam	Longitudinal Reinforcement			Shear Reinforcement		a/d	d (in)
	Bars	Reinforcement ratio (%)	f_y (ksi)	Bars	f_{yv} (ksi)		
N1	3#8	1.48	60	-	-	2.5	16
N2	3#8	1.48	60	-	-	2.5	16
A1	3#8	1.48	60	#2 @ 7.5" c/c	40	2.5	16
A2	3#8	1.48	60	#2 @ 7.5" c/c	40	2.5	16
Z1	3#8	1.48	60	#3 @ 6" c/c	40	2.5	16
Z2	3#8	1.48	60	#3 @ 6" c/c	40	2.5	16
M1	3#8	1.48	60	#3 @ 8" c/c	40	2.5	16
M2	3#8	1.48	60	#3 @ 8" c/c	40	2.5	16

5.1 Comparison of ultimate shear strength predicted by ACI and FEM

The Comparison of ultimate shear strength predicted by ACI and FEM have been shown in the tables as follows:

Table 5.2: Experimental Comparison of results between (Kashif, 2014) and ABAQUS (FEM) for shear span-to-depth ratio of 2.5

Beam $\frac{a}{d} = 2.5$	Experimental Strength, KN			ACI Predicted Strength, KN			FEM Predicted Strength, KN			$\frac{V_u(exp)}{V_u(ACI)}$	$\frac{V_u(exp)}{V_u(FEM)}$	$\frac{V_u(FEM)}{V_u(ACI)}$	α
	Vc	Vs	Vu	Vc	Vs	Vu	Vc	Vs	Vu				
N1	123	0	123	92	0	92	108	0	108	1.33	1.13	1.17	2.4
N2	123	0	123	92	0	92	108	0	108	1.33	1.13	1.17	2.4
Mean Value	123	0	123	92	0	92	108	0	108	1.33	1.13	1.17	2.4
A1	166	37	203	92	37	129	111	56	167	1.57	1.21	1.29	2.47
A2	171	37	209	92	37	129	111	56	167	1.62	1.25	1.29	2.47
Mean Value	169	37	206	92	37	129	111	56	167	1.59	1.23	1.29	2.47
Z1	185	105	290	92	105	197	113	122	235	1.47	1.23	1.20	2.53
Z2	184	105	288	92	105	197	113	122	235	1.47	1.23	1.20	2.53
Mean Value	185	105	289	92	105	197	113	122	235	1.47	1.23	1.20	2.53
M1	165	78	243	92	78	170	112	85	197	1.43	1.23	1.15	2.51
M2	159	78	237	92	78	170	112	85	197	1.39	1.2	1.16	2.51
Mean Value	162	78	240	92	78	170	112	85	197	1.41	1.22	1.16	2.51
Total Mean			215			147			177	1.45	1.21	1.2	2.475
Variation										45%	21%	20%	

Where α is a factor which is studied in this research and its implication on varying shear span to depth is studied.

$$V_u = V_c + V_s$$

$$V_c = \alpha \sqrt{f'c} b_w d$$

$$V_u = \alpha \sqrt{f'c} b_w d + V_s$$

Table 5.3: Comparison of results between ACI and ABAQUS (FEM) for shear span-to-depth ratio of 3

Beam (a/d = 3)	ACI Predicted Strength, KN			FEM Predicted Strength, KN			$\frac{V_u(FEM)}{V_u(ACI)}$	α
	V_c	V_s	V_u	V_c	V_s	V_u		
N	92	0	92	106	0	106	1.15	2.37
A	92	37	129	108	56	164	1.27	2.39
Z	92	105	197	109	122	231	1.17	2.42
M	92	78	170	107	85	192	1.12	2.41
Total Mean			147			173	1.18	2.39

Table 5.4: Comparison of results between ACI and ABAQUS (FEM) for shear span-to-depth ratio of 3.5

Beam (a/d = 3.5)	ACI Predicted Strength, KN			FEM Predicted Strength, KN			$\frac{V_u(FEM)}{V_u(ACI)}$	α
	V_c	V_s	V_u	V_c	V_s	V_u		
N	92	0	92	101	0	101	1.1	2.24
A	92	37	129	102	56	158	1.22	2.27
Z	92	105	197	104	122	226	1.14	2.3
M	92	78	170	103	85	188	1.11	2.28
Total Mean			147			168.25	1.143	2.27

Table 5.5: Comparison of results between ACI and ABAQUS (FEM) for shear span-to-depth ratio of 4.0

Beam ($a/d = 4$)	ACI Predicted Strength, KN			FEM Predicted Strength, KN			$\frac{V_u(FEM)}{V_u(ACI)}$	α
	V_c	V_s	V_u	V_c	V_s	V_u		
N	92	0	92	95	0	95	1.03	2.1
A	92	37	129	98	56	158	1.22	2.18
Z	92	105	197	108	122	230	1.16	2.4
M	92	78	170	99	85	184	1.02	2.2
Total Mean			147			166.75	1.1	2.2

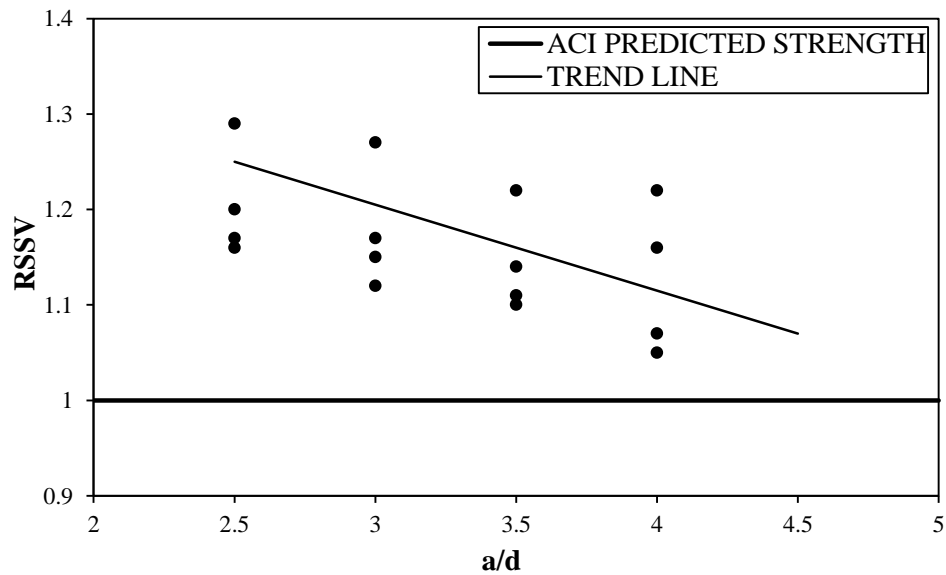


Fig 5.1: Change in RSSV and its trend with increasing a/d ratio

*RSSV = Relative Shear Strength value of the ratio $\frac{V_{fail}}{V_{predicted}}$

The values from the graph and table indicates that with the increase in the shear span to depth ratio between 2.5 to 4 the ultimate strength of beam in shear decreases. As the trend line shows, there is a drop of around 5% in the values of strength.

Moreover, in comparison with the ACI predicted strength, it can be seen that the values suggested by numerical modelling are slightly higher than those predicted. This is because the ACI under predicts the strength due to the fact that all factors have not been fully incorporated which leads to the conservativeness of the shear design given by ACI.

To address this issue of conservativeness, a new modification in Zararis equation is presented that incorporates additional factors to predict the shear strength. As established before, Zararis suggest an additional parameter as splitting length l_t which depended upon ΔV_d . He asserted that this splitting length is a function of the depth. However, for this research, the assumption made by Kashif is considered more rational, as he considers this splitting length as a function of development length. The next section shows the modified equation to predict the ultimate shear strength.

$$V_u = \left[\left(1.2 - 0.2 \frac{a}{d} \right) \frac{c}{d} f_{ct} + 0.21 \left(\left(\frac{l_d}{d} \right) + 0.25 \left(\frac{a}{d} \right) \right) \rho_v f_{yv} \right] bd$$

Using the above proposed equation it is found out that it gives a better strength prediction and the values are found closer to those of the finite element model as shown in the table and graph below.

Table 5.6: Comparison of results of Shear Strength predicted between ACI and modified equation

a/d	Equation Predicted Strength,	ACI Predicted Strength,	(RSSV)* Ratio
	KN V_u	KN V_u	
2.5	161.7	147	1.1
3	157.3	147	1.07
3.5	154.4	147	1.05
4	152.9	147	1.04

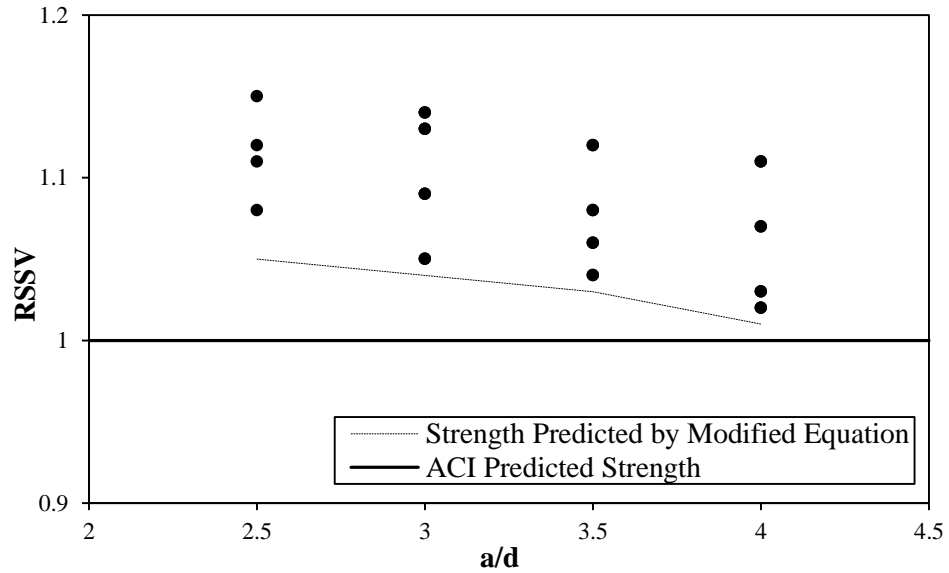


Figure 5.2: Improved results of the modified equation as compared to ACI, this predicted line corresponds to less conservative results

$$*RSSV = \text{Relative Shear Strength value of the ratio } \frac{V_{fail}}{V_{predicted}}$$

And to conclude this research, an expression for minimum amount of shear reinforcement for attainment of nominal flexural capacity is also presented and is written below.

$$\rho_v = \frac{1}{f_{yv}} \left[\frac{\rho f_y}{(a/d)} \left(1 - \frac{\rho f_y}{1.7 f_c} \right) - \alpha \sqrt{f_c} \right]$$

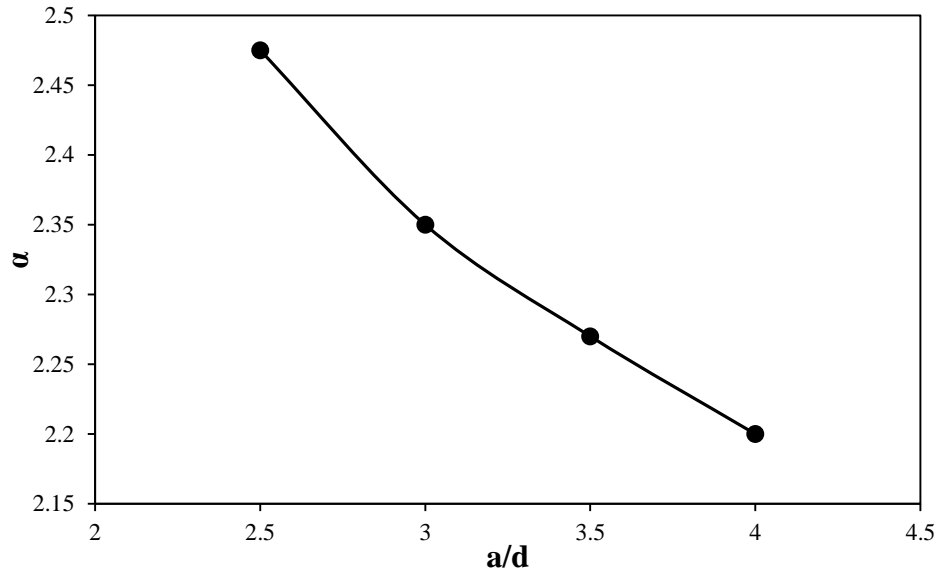


Figure 5.3: The variation in value of α with the increase in a/d ratio

5.2 Cracking Pattern of the modelled beams

The cracking pattern was visualized using the vector plot of plastic strains in ABAQUS using PEMAG function. Although this is not the most recommended method available, but it can still give a qualitative idea as to what cracking patterns are expected.

5.2.1 General Cracking Pattern

1. For beams without web reinforcement the presence of inclined cracks is more prominent compared to the flexure cracks.
2. For beams with shear reinforcement, the presence of flexure cracks was observed along with some inclined cracking.
3. With the increase in shear span, flexure failure is expected and this is represented by an increased number of flexure cracks for a/d ratios of 3.5 and 4.0.

5.3 Beams with Shear Span to Depth Ratio 2.5

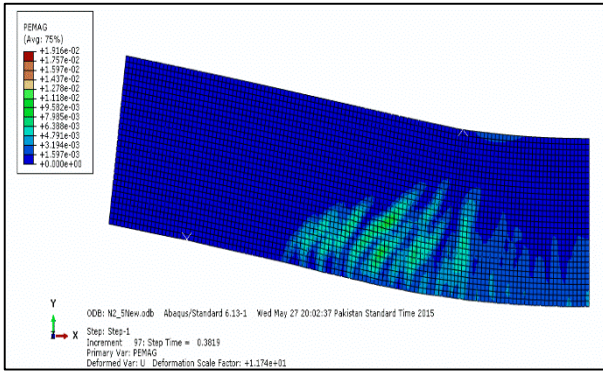


Fig 5.4: Inclined Cracking more prominent for beams w/o web reinforcement for Beam N1 with $a/d = 2.5$

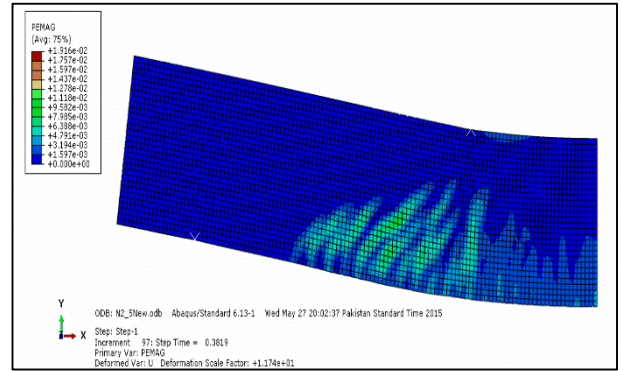


Fig 5.5: Inclined cracking more prominent for beams w/o web reinforcement for Beam N2 with $a/d = 2.5$

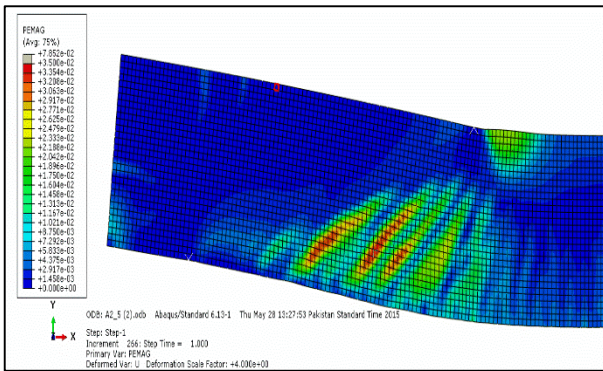


Fig 5.6: Presence of vertical ties addresses some of the diagonal cracks. However due to shorter moment arm lesser flexure cracks appear for Beam A1 with $a/d = 2.5$

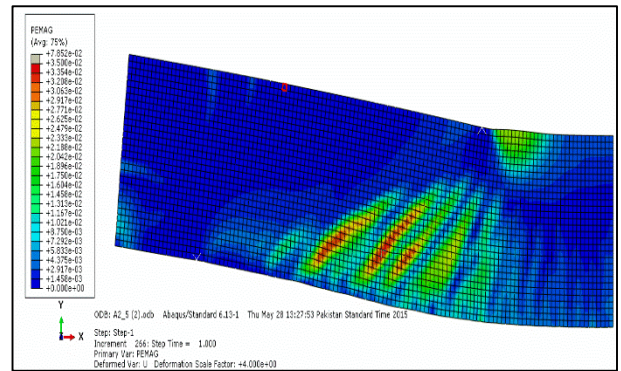


Fig 5.7: Presence of vertical ties addresses some of the diagonal cracks. However due to shorter moment arm lesser flexure cracks appear for Beam A2 with $a/d = 2.5$

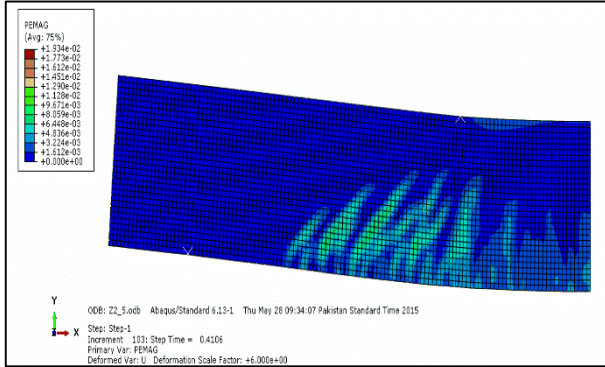


Fig 5.8: Both flexure and shear cracks appear for Beam Z1 with $a/d = 2.5$

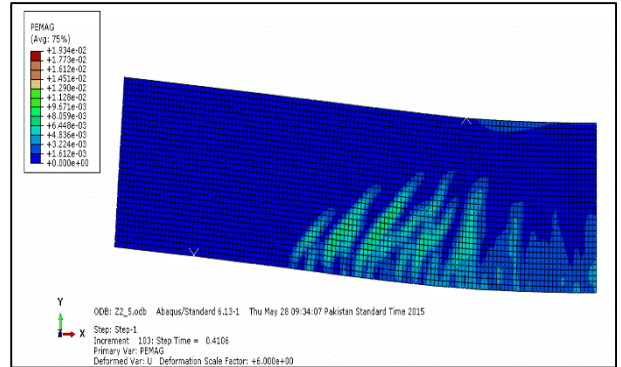


Fig 5.9: Both flexure and shear cracks appear for Beam Z2 with $a/d = 2.5$

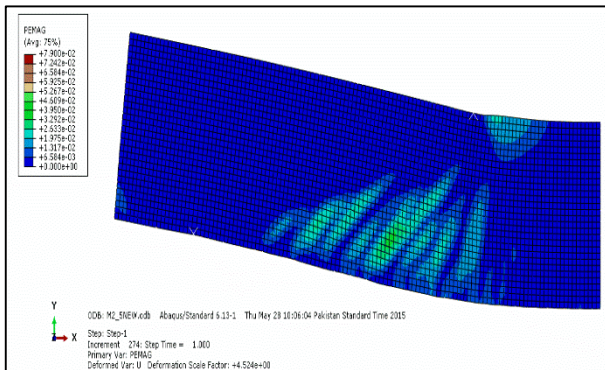


Fig 5.10: Lesser Flexure cracks compared to the inclined cracks for Beam M1 with $a/d = 2.5$. Some crushing of concrete is also observed at the loading point.

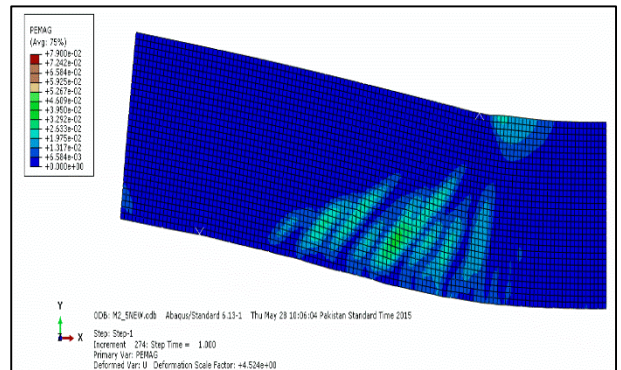


Fig 5.11: Lesser Flexure cracks compared to the inclined cracks for Beam M2 with $a/d = 2.5$. Some crushing of concrete is also observed at the loading point

5.5 Beams with Shear Span to Depth Ratio of 3.5

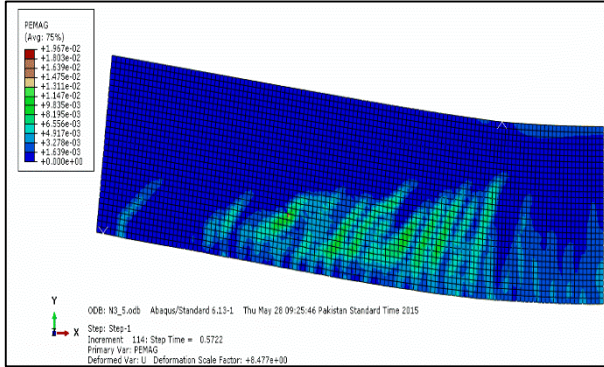


Fig 5.16: As the shear span increases further, number of flexure cracks increase in number. Some flexure cracks also appear for Beam N4 with a/d of 3.5

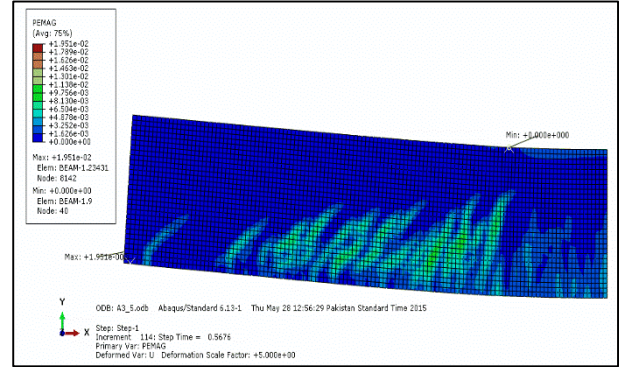


Fig 5.17: More flexure cracks compared to Shear Span of 3.0 for beam A4 with a/d of 3.5

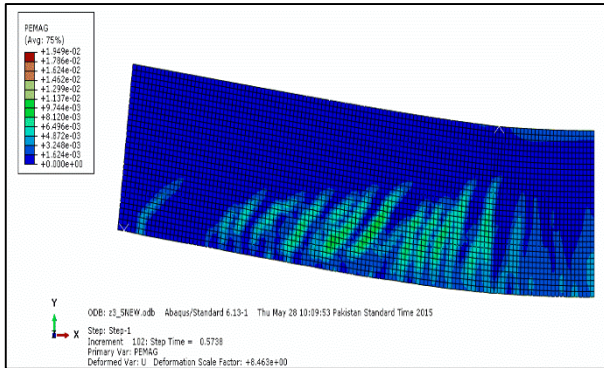


Fig 5.18: With the increase in Shear Span, the presence of more flexure cracks is justified, Beam Z4 with a/d of 3.5

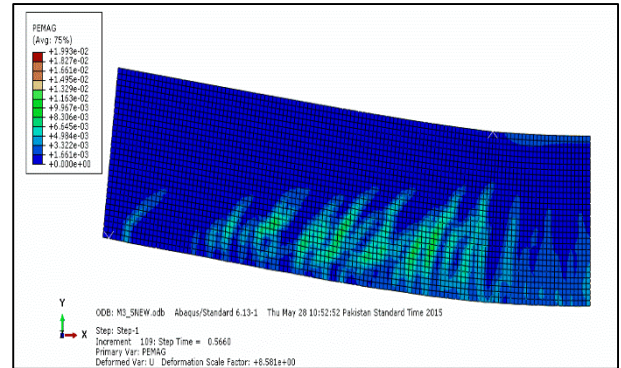


Fig 5.19: Flexure Cracks increase with the increase in shear span, Beam M4 with a/d of 3.5

5.6 Beams with Shear Span to Depth Ratio of 4.0

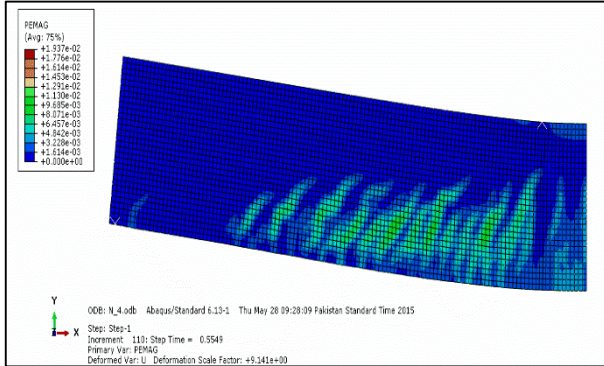


Fig 5.20: Flexural Crack more dominant than the shear inclined cracks for the Beam N5 with a/d of 4.0

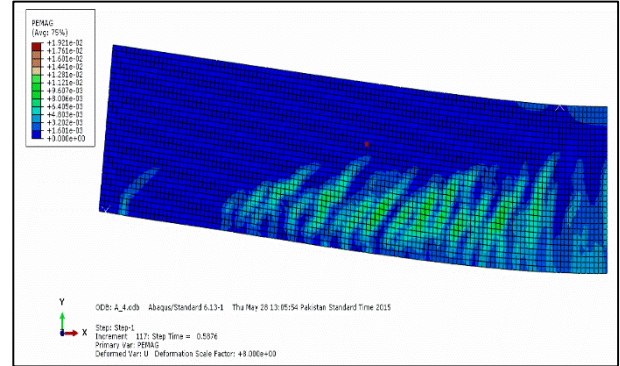


Fig 5.21: More Flexural cracks compared to Shear span of 3.5, A5 is justified with a/d of 4.0

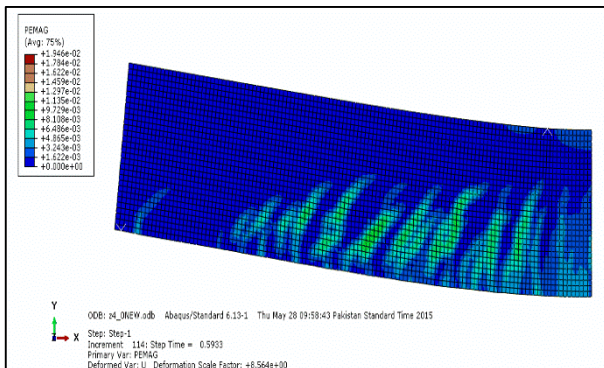


Fig 5.22: With the increase in Shear Span, the presence of more flexure cracks is justified for Z5 with a/d of

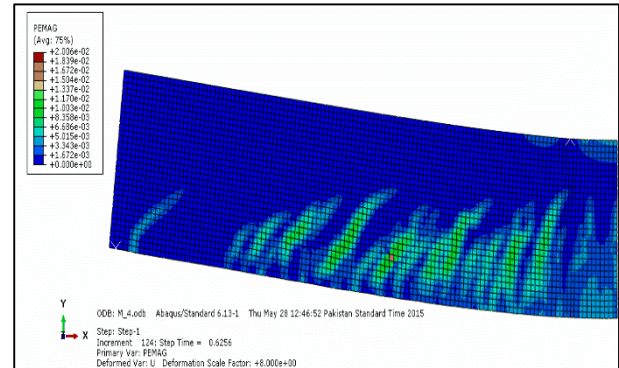


Fig 5.23: Flexure Cracks increase with the increase in shear span for beam M5 with a/d of 4.0

DERIVATION OF MODIFIED EQUATIONS

6.1 Equations for Ultimate Shear Strength and Minimum Shear Reinforcement

Zararis's expression for ΔV_d (discussed earlier) is as follows:

$$\Delta V_d = 0.5 \rho_v f_{yv} b d$$

Taking into account, a new factor called development length (l_d); which previous researchers believe to influence the Ultimate Shear Strength of RC beams. This factor is believe to alter the splitting length of concrete along the main horizontal reinforcement. This horizontal splitting leads to immediate failure in shear as dowel action force drops to zero. Realizing the factor's influence, modification to the above expression is as follows where splitting length is taken as $l_t = 0.25 l_d$

$$\Delta V_d = 0.25 \frac{l_d}{d} \rho_v f_{yv} b d$$

Substituting this new expression in following equation

$$V_u = V_{cr} + V_s + \Delta V_d$$

Results in a final modified equation for ultimate shear strength of RC Slender beams

$$V_u = \left[\left(1.2 - 0.2 \frac{a}{d} \right) \frac{c}{d} f_{ct} + 0.21 \left(\left(\frac{l_d}{d} \right) + 0.25 \left(\frac{a}{d} \right) \right) \rho_v f_{yv} \right] b d$$

Taking this concept further, in order to devise another modified equation for minimum shear provision, ΔV_d is substituted to Eq.4 (2.10.3) results in an improved equation as under:

$$\frac{\rho}{\rho_v} \leq 0.89 \frac{l_d}{d} \left(\frac{a}{d} \right)$$

6.2 Derivation of Minimum Shear Reinforcement which ascertains full flexure capacity

$$V_u \times a' = A_s f_y \left(d - \frac{a}{2} \right)$$

a' represents *shear span*

$$V_u = \frac{A_s f_y}{a'} d \left(1 - \frac{a}{2d} \right)$$

$$V_u = \frac{A_s f_y}{\left(\frac{a'}{d} \right)} \left[1 - \frac{A_s f_y}{1.7 f'_c \times b d} \right]$$

$$V_u = \frac{A_s f_y}{\left(\frac{a'}{d} \right)} \left(1 - \frac{\rho f_y}{1.7 f'_c} \right)$$

$$\therefore a = \frac{A_s f_y}{0.85 f'_c \times b}$$

Both concrete and steel superposed strengths results in total shear strength,

$$V_c + V_s = \frac{A_s f_y}{\left(\frac{a'}{d} \right)} \left(1 - \frac{\rho f_y}{1.7 f'_c} \right)$$

$$V_s = \frac{A_s f_y}{\left(\frac{a'}{d} \right)} \left(1 - \frac{\rho f_y}{1.7 f'_c} \right) - V_c$$

Using ACI-318-(11.13 and 11.15) equations for v_s and v_c :

$$\frac{A_v f_{yv} d}{s} = \frac{A_s f_y}{\left(\frac{a'}{d}\right)} \left(1 - \frac{\rho f_y}{1.7 f_c}\right) - \alpha \sqrt{f_c} b d$$

$$\frac{A_v f_{yv}}{b s} = \frac{A_s f_y}{b d \left(\frac{a'}{d}\right)} \left(1 - \frac{\rho f_y}{1.7 f_c}\right) - \alpha \sqrt{f_c}$$

$$\rho_v f_{yv} = \frac{\rho f_y}{\left(\frac{a'}{d}\right)} \left(1 - \frac{\rho f_y}{1.7 f_c}\right) - \alpha \sqrt{f_c}$$

And to conclude this research, an expression for minimum amount of shear reinforcement for attainment of nominal flexural capacity is also presented and is written below.

$$\rho_v = \frac{1}{f_{yv}} \left[\frac{\rho f_y}{\left(\frac{a'}{d}\right)} \left(1 - \frac{\rho f_y}{1.7 f_c}\right) - \alpha \sqrt{f_c} \right]$$

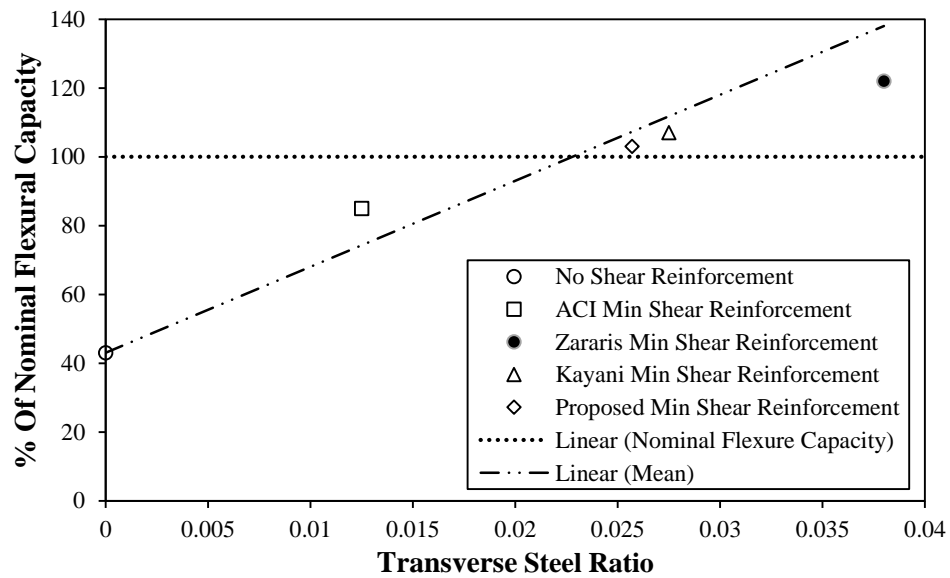


Figure 6.1: Relation of %Nominal Capacity to Transverse Reinforcement Ratio.

It can be clearly seen that the proposed equation for minimum reinforcement provides the best prediction.

CONCLUSIONS AND RECOMMENDATION

7.1 Conclusions

At the end conclusion devised by our team and the conclusions that we reached are as follows

1. Finite Element Modelling (FEM) is a technique which can be used to better understand shear failure mechanism.
2. FEM significantly reduces time and effort in comparison to experimental testing
3. The equation devised by Kayani et al. provides a better shear strength prediction than ACI
4. The proposed equation provides better prediction for full flexure capacity of RC beams

7.3 Recommendations

1. More experimental work needed to calibrate the material model as per the local conditions.
2. The effect of shear span to depth ratio in slender beams with stirrups needs to be validated with further experimental study.
3. Advanced crack detection and evolution techniques such as XFEM, VCCT and VUMAT can help a better prediction of cracks, unlike the qualitative technique used in this research.

APPENDIX

Table 1: Beam N1 Experimental and FEM Model's Load Deflection Comparison

Experimental				Model			
Load (Ton)	Deflections (mm)			Load (Ton)	Deflections (mm)		
	Quarter Point	Mid-Point	Quarter Point		Quarter Point	Mid-Point	Quarter Point
0.00	0.00	0.00	0	0.00	0.00	0.00	0.00
2.50	0.56	0.66	0.56	2.50	0.45	0.58	0.45
5.00	1.04	1.45	1.07	5.00	0.95	1.15	0.95
7.50	1.57	1.91	1.57	7.50	1.48	1.73	1.48
10.00	2.36	2.79	2.21	10.00	1.98	2.30	1.98
12.50	3.05	3.35	2.67	12.50	2.47	2.90	2.47
15.00	3.45	4.06	3.28	15.00	2.97	3.53	2.97
17.50	4.24	4.90	3.99	17.50	3.47	4.15	3.47
20.00	4.83	5.51	4.47	20.00	3.98	4.78	3.98
22.50	5.54	6.27	5.03	22.50	4.56	5.48	4.56
25.00	7.32	7.62	5.72	25.00	5.38	6.90	5.38
27.50	7.84	8.21	7.98	27.00	6.35	7.70	6.35
20.00	6.99	8.61	7.22	27.10	6.85	9.56	6.85
16.00	5.91	8.45	6.56	26.40	9.00	12.32	9.00
14.50	5.49	7.75	6.35	25.10	10.10	13.01	10.10
10.00	4.78	7.01	5.97	22.90	12.01	14.50	12.01
6.00	4.03	6.13	5.54				
4.00	3.18	5.74	4.86				
2.50	2.96	4.97	4.29				
0.05	2.33	4.29	3.51				

Table 2: Beam N2 Experimental and FEM Model's Load Deflection comparison

Experimental				Model			
Load (Ton)	Deflections (mm)			Load (Ton)	Deflections (mm)		
	Quarter Point	Mid-Point	Quarter Point		Quarter Point	Mid-Point	Quarter Point
0.00	0.00	0.00	0.00	0.00	0.00	0.00	0.00
2.50	0.33	0.55	0.82	2.50	0.45	0.58	0.45
5.00	0.74	1.21	1.80	5.00	0.95	1.15	0.95
7.50	1.23	2.02	2.20	7.50	1.48	1.73	1.48
10.00	1.81	3.00	2.81	10.00	1.98	2.30	1.98
12.50	2.38	3.88	4.04	12.50	2.47	2.90	2.47
15.00	2.89	4.68	5.16	15.00	2.97	3.53	2.97
17.50	3.49	5.56	6.45	17.50	3.47	4.15	3.47
20.00	4.11	6.46	7.76	20.00	3.98	4.78	3.98
22.50	5.35	7.56	9.46	22.50	4.56	5.48	4.56
25.00	5.69	8.07	10.21	25.00	5.38	6.90	5.38
21.50	6.00	8.98	13.83	27.00	6.35	7.70	6.35
20.00	6.09	9.31	15.22	27.10	6.85	9.56	6.85
17.20	5.75	8.82	14.56	26.40	9.00	12.32	9.00
14.80	5.39	8.25	13.63	25.10	10.10	13.01	10.10
10.75	4.69	7.16	11.82	22.90	12.01	14.50	12.01
8.00	4.17	6.37	10.50				
4.00	3.34	5.13	8.39				
2.33	2.85	4.44	7.15				
0.02	2.13	3.39	5.31				

Table 3: Beam A1 Experimental and FEM Model's Load Deflection comparison

Experimental				Model			
Load (Ton)	Deflections (mm)			Load (Ton)	Deflections (mm)		
	Quarter Point	Mid-Point	Quarter Point		Quarter Point	Mid-Point	Quarter Point
0.00	0.00	0.00	0.00	0.00	0	0.00	0
0.00	0.00	0.00	0.00	2.50	0.20	0.33	0.20
2.50	0.56	0.66	0.56	5.00	0.40	0.67	0.40
5.00	1.04	1.45	1.07	7.50	0.74	1.17	0.74
7.50	1.57	1.91	1.57	10.00	1.09	1.79	1.09
10.00	2.36	2.79	2.21	12.50	1.60	2.42	1.60
12.50	3.05	3.35	2.67	15.00	2.00	3.05	2.00
15.00	3.45	4.06	3.28	17.50	2.52	3.70	2.52
17.50	4.24	4.90	3.99	20.00	2.88	4.35	2.88
20.00	4.83	5.51	4.47	22.50	3.15	5.01	3.15
22.50	5.54	6.27	5.03	25.00	4.34	6.13	4.34
25.00	7.32	7.62	5.72	27.50	5.11	7.04	5.11
27.50	7.84	8.21	7.98	30.00	5.64	7.76	5.64
20.00	6.99	8.61	7.22	32.50	6.27	8.53	6.27
16.00	5.91	8.45	6.56	35.00	7.26	9.67	7.26
14.50	5.49	7.75	6.35	37.50	8.00	10.60	8.00
10.00	4.78	7.01	5.97	40.00	11.42	14.17	11.42
6.00	4.03	6.13	5.54	40.1	11.60	14.4	11.60
4.00	3.18	5.74	4.86	39.00	12.89	15.77	12.89
2.50	2.96	4.97	4.29	37.50	13.47	16.73	13.47
0.05	2.33	4.29	3.51	36.00	11.69	17.24	11.69
				32.50	12.44	18.60	12.44
				27.50	14.11	20.10	14.11

Table 4: Beam A2 Experimental and FEM Model's Load Deflection comparison

Experimental				Model			
Load (Ton)	Deflections (mm)			Load (Ton)	Deflections (mm)		
	Quarter Point	Mid- Point	Quarter Point		Quarter Point	Mid- Point	Quarter Point
0.00	0.00	0.00	0.00	0.00	0	0.00	0
2.46	0.10	0.54	0.39	2.50	0.20	0.33	0.20
4.91	0.40	1.00	0.81	5.00	0.40	0.67	0.40
7.46	0.74	1.57	1.26	7.50	0.74	1.17	0.74
9.82	1.26	2.44	1.91	10.00	1.09	1.79	1.09
12.32	1.65	3.05	2.43	12.50	1.60	2.42	1.60
14.78	2.12	3.79	3.00	15.00	2.00	3.05	2.00
17.23	2.59	4.49	3.57	17.50	2.52	3.70	2.52
19.69	3.02	5.11	4.08	20.00	2.88	4.35	2.88
22.14	3.68	6.00	4.88	22.50	3.15	5.01	3.15
24.60	5.12	7.50	6.08	25.00	4.34	6.13	4.34
27.05	5.42	7.92	6.43	27.50	5.11	7.04	5.11
29.51	6.31	9.22	7.74	30.00	5.64	7.76	5.64
31.96	6.74	9.85	8.31	32.50	6.27	8.53	6.27
34.42	7.52	10.92	9.28	35.00	7.26	9.67	7.26
36.92	8.10	11.70	9.96	37.50	8.00	10.60	8.00
39.38	9.37	13.27	11.40	40.00	11.42	14.17	11.42
41.83	10.31	14.36	12.34	40.1	11.60	14.4	11.60
40.85	10.57	14.50	12.39	39.00	12.89	15.77	12.89
32.28	13.29	16.57	12.96	37.50	13.47	16.73	13.47
26.25	14.77	17.39	13.18	36.00	11.69	17.24	11.69
25.49	15.31	17.53	13.18	32.50	12.44	18.60	12.44
11.29	11.67	14.64	10.10	27.50	14.11	20.10	14.11
2.46	7.13	10.08	7.42				
0.00	6.54	8.34	6.14				

Table 5: Beam Z1 Experimental and FEM Model's Load Deflection comparison

Experimental				Model			
Load (Ton)	Deflections (mm)			Load (Ton)	Deflections (mm)		
	Quarter Point	Mid-Point	Quarter Point		Quarter Point	Mid-Point	Quarter Point
0.00	0.00	0.00	0.00	0.00	0	0	0
2.50	0.37	0.59	0.47	2.50	0.57	0.58	0.57
5.00	0.95	1.23	0.96	5.00	1.03	1.16	1.03
7.50	1.41	1.87	1.43	7.50	1.49	1.73	1.49
10.00	2.15	2.93	2.21	10.00	1.95	2.31	1.95
12.50	2.92	3.97	3.00	12.50	2.43	2.92	2.43
15.00	3.26	4.45	3.37	15.00	2.91	3.54	2.91
17.50	3.85	5.11	3.97	17.50	3.39	4.18	3.39
20.00	4.67	6.18	4.81	20.00	3.87	4.8	3.87
22.50	5.07	6.71	5.22	22.50	4.34	5.74	4.34
25.00	5.55	7.38	5.76	25.00	4.82	6.59	4.82
27.50	6.40	8.46	6.64	27.50	5.49	7.45	5.49
30.00	7.27	9.63	7.72	30.00	6.16	8.31	6.16
32.50	7.82	10.39	8.31	32.50	6.84	9.18	6.84
35.00	8.31	11.08	8.85	35.00	7.53	10.08	7.53
37.50	9.05	12.10	9.63	37.50	8.26	10.98	8.26
40.00	9.72	12.97	10.31	40.00	9.01	11.88	9.01
42.50	10.46	13.99	11.08	42.50	9.88	12.77	9.88
45.00	11.18	15.01	11.89	45.00	10.78	13.67	10.78
47.50	12.51	16.15	12.78	47.50	11.72	14.57	11.72
50.00	13.49	17.56	13.90	50.00	12.88	15.46	12.88
52.50	14.04	18.35	14.47	52.50	14.25	16.67	14.25
55.00	15.43	19.73	15.50	55.00	16.2	17.87	16.2
57.50	16.57	21.17	16.58	57.50	19.2	18.96	19.2
58.93	17.14	22.02	17.18	58.93	20.3	19.58	20.3
57.53	17.33	22.32	17.31	59.12	21.7	19.67	21.7
59.12	18.61	24.08	18.41	59.20	22.4	19.7	22.4
57.60	23.41	30.10	21.47	62.10	23.3	22	23.3
52.80	24.17	31.68	22.08	62.80	23.41	24.1	23.41
46.89	23.55	31.40	21.47	62.70	24.78	25.4	24.78
41.89	22.80	30.31	20.73	62.20	25.86	27.4	25.86
37.18	22.00	29.19	19.89	61.20	26	28.6	26
31.28	20.87	27.60	18.71	57.60	27.32	30.88	27.32
28.13	20.24	26.68	18.04	52.80	29.42	32.16	29.42
23.75	19.30	25.32	17.04	46.89	30.02	33.14	30.02
18.86	18.27	23.83	15.94	37.18	31.33	34	31.33
15.16	17.29	22.46	14.92				
9.60	16.00	20.53	13.47				
3.34	14.08	17.75	11.26				
1.07	13.12	16.45	10.25				
0.25	12.67	15.87	9.81				
0.04	12.05	15.18	9.14				

Table 6: Beam Z2 Experimental and FEM Model's Load Deflection comparison

Experimental				Model			
Load (Ton)	Deflections (mm)			Load (Ton)	Deflections (mm)		
	Quarter Point	Mid - Point	Quarter Point		Quarter Point	Mid-Point	Quarter Point
0.00	0.00	0.00	0.00	0.00	0	0	0
2.50	0.48	0.60	0.46	2.50	0.57	0.58	0.57
5.00	1.08	1.32	0.96	5.00	1.03	1.16	1.03
7.50	1.59	2.02	1.44	7.50	1.49	1.73	1.49
10.00	2.46	3.20	2.29	10.00	1.95	2.31	1.95
12.50	2.96	3.89	2.81	12.50	2.43	2.92	2.43
15.00	3.57	4.76	3.47	15.00	2.91	3.54	2.91
17.50	4.24	5.66	4.19	17.50	3.39	4.18	3.39
20.00	4.89	6.55	4.91	20.00	3.87	4.8	3.87
22.50	5.64	7.47	5.66	22.50	4.34	5.74	4.34
25.00	6.31	8.30	6.32	25.00	4.82	6.59	4.82
27.50	7.27	9.47	7.28	27.50	5.49	7.45	5.49
30.00	7.88	10.33	8.01	30.00	6.16	8.31	6.16
32.50	8.52	11.26	8.85	32.50	6.84	9.18	6.84
35.00	9.19	12.19	9.62	35.00	7.53	10.08	7.53
37.50	10.19	13.56	10.77	37.50	8.26	10.98	8.26
40.00	10.56	14.10	11.19	40.00	9.01	11.88	9.01
42.50	11.28	14.87	11.83	42.50	9.88	12.77	9.88
45.00	12.00	15.90	12.69	45.00	10.78	13.67	10.78
47.50	12.71	16.91	13.54	47.50	11.72	14.57	11.72
50.00	13.94	18.23	14.63	50.00	12.88	15.46	12.88
52.50	14.63	19.22	15.42	52.50	14.25	16.67	14.25
55.00	15.70	20.76	16.63	55.00	16.2	17.87	16.2
57.50	20.13	25.25	19.60	57.50	19.2	18.96	19.2
58.93	20.99	26.23	20.20	58.93	20.3	19.58	20.3
55.00	22.06	26.88	20.42	59.12	21.7	19.67	21.7
47.00	29.58	31.82	22.65	59.20	22.4	19.7	22.4
42.00	28.87	30.63	21.82	62.10	23.3	22	23.3
36.00	27.75	29.02	20.61	62.80	23.41	24.1	23.41
27.84	25.99	26.65	18.75	62.70	24.78	25.4	24.78
25.24	25.41	25.86	18.14	62.20	25.86	27.4	25.86
19.64	24.12	24.14	16.79	61.20	26	28.6	26
16.15	23.22	22.93	15.85	57.60	27.32	30.88	27.32
13.91	22.68	22.18	15.27	52.80	29.42	32.16	29.42
11.91	22.05	21.42	14.66	46.89	30.02	33.14	30.02
7.33	20.52	19.67	13.28	37.18	31.33	34	31.33
5.09	19.73	18.75	12.57				
2.76	18.64	17.60	11.65				
0.09	16.99	16.01	10.41				

Table 7: Beam M1 Experimental and FEM Load's Deflection comparison

Experimental				Model			
Load (Ton)	Deflections (mm)			Load (tonnes)	Deflections (mm)		
	Quarter Point	Mid-Point	Quarter Point		Quarter Point	Mid-Point	Quarter Point
0.00	0.00	0.00	0.00	0.00	0.00	0.00	0.00
2.50	0.40	0.66	0.48	2.50	0.35	0.37	0.35
5.00	0.98	1.47	0.91	5.00	0.78	0.83	0.78
7.50	1.24	2.02	1.57	7.50	1.16	1.34	1.16
10.00	1.84	2.97	2.07	10.00	1.55	1.94	1.55
12.50	2.41	3.88	2.65	12.50	1.93	2.75	1.93
15.00	3.01	4.75	3.16	15.00	2.46	3.34	2.46
17.50	3.61	5.56	3.93	17.50	3.09	4.01	3.09
20.00	4.39	6.67	4.80	20.00	3.78	4.75	3.78
23.50	5.14	7.82	5.76	23.50	4.74	5.80	4.74
25.00	5.54	8.39	6.62	25.00	5.15	6.28	5.15
27.50	6.42	9.66	8.69	27.50	5.91	7.08	5.91
30.00	7.29	10.88	10.45	30.00	6.70	7.97	6.70
32.50	7.82	11.62	11.51	32.50	7.55	8.88	7.55
35.00	8.59	12.71	13.07	35.00	8.46	10.06	8.46
37.50	9.11	13.47	14.14	37.50	9.52	11.21	9.52
40.00	9.95	14.68	15.87	40.00	10.65	12.53	10.65
42.50	11.27	15.85	17.56	42.50	12.18	14.10	12.18
45.00	11.85	16.92	19.09	45.00	13.91	15.82	13.91
47.50	11.92	17.77	20.35	47.50	15.79	17.43	15.79
49.50	11.87	18.35	21.21	49.50	17.45	18.82	17.45
50.50	12.87	19.35	22.21	50.20	17.57	19.40	17.57
51.50	13.87	20.35	23.21	50.40	17.96	20.40	17.96
				51.2	18.9	21.32	18.90
				52.7	20.4	22.69	20.40
				51.8	21.5	21.5	21.50
				48.08	22.54	23.07	22.54
				47.5	23.2	24.09	23.20
				45.93	23.87	24.31	23.87
				42.3	24.7	25.54	24.70

Table 8: Beam M2 Experimental and FEM Model's Load Deflection comparison

Experimental				Model			
Load (Ton)	Deflections (mm)			Load (tones)	Deflections (mm)		
	Quarter Point	Mid-Point	Quarter Point		Quarter Point	Mid-Point	Quarter Point
0.00	0.00	0.00	0.00	0.00	0.00	0.00	0.00
2.50	0.59	0.60	0.43	2.50	0.35	0.37	0.35
5.00	1.19	1.40	1.00	5.00	0.78	0.83	0.78
7.52	1.85	2.35	1.66	7.50	1.16	1.34	1.16
10.02	2.39	3.14	2.24	10.00	1.55	1.94	1.55
12.50	3.02	4.04	2.90	12.50	1.93	2.75	1.93
15.07	3.60	4.83	3.50	15.00	2.46	3.34	2.46
17.52	4.17	5.64	4.09	17.50	3.09	4.01	3.09
20.08	5.01	6.77	5.02	20.00	3.78	4.75	3.78
22.53	5.84	7.87	5.85	23.50	4.74	5.80	4.74
25.07	6.38	8.66	6.43	25.00	5.15	6.28	5.15
27.51	7.21	9.84	7.38	27.50	5.91	7.08	5.91
30.05	7.94	10.92	8.24	30.00	6.70	7.97	6.70
32.50	8.38	11.54	8.74	32.50	7.55	8.88	7.55
35.08	9.29	12.88	9.84	35.00	8.46	10.06	8.46
37.57	10.10	14.06	10.81	37.50	9.52	11.21	9.52
40.01	10.78	15.02	11.57	40.00	10.65	12.53	10.65
42.52	11.53	16.09	12.46	42.50	12.18	14.10	12.18
45.00	12.39	17.30	13.44	45.00	13.91	15.82	13.91
47.51	13.52	19.14	15.30	47.50	15.79	17.43	15.79
48.41	13.83	19.66	15.84	49.50	17.45	18.82	17.45
48.08	13.84	19.71	15.93	50.20	17.57	19.40	17.57
45.93	13.89	20.08	16.58	50.40	17.96	20.40	17.96
42.44	13.98	20.68	17.73	51.2	18.9	21.32	18.90
40.78	14.01	20.92	18.32	52.7	20.4	22.69	20.40
36.73	13.43	20.03	17.67	51.8	21.5	21.5	21.50
31.55	12.60	18.75	16.72	48.08	22.54	23.07	22.54
21.79	10.81	16.01	14.67	47.5	23.2	24.09	23.20
13.25	8.98	13.26	12.48	45.93	23.87	24.31	23.87
6.33	7.23	10.61	10.29	42.3	24.7	25.54	24.70
2.16	5.87	8.58	8.64				
0.02	4.86	6.87	7.34				

BIBLIOGRAPHY

ACI (2008). Building Code Requirements for Structural Concrete (ACI 318-08) and Commentary, American Concrete Institute.

Ahamad, S. H., et al. (1994). "Shear strength of reinforced lightweight concrete beams of normal and high strength concrete." Magazine of Concrete Research **46**(166): 57-66.

Anderson, N. S. and J. A. Ramirez (1989). "Detailing of stirrup reinforcement." ACI Structural Journal **86**(5): 507-515.

Angelakos, D., et al. (2001). "Effect of concrete strength and minimum stirrups on shear strength of large members." ACI Structural Journal **98**(3).

Bresler, B. and A. C. Scordelis (1963). Shear strength of reinforced concrete beams. ACI Journal Proceedings, ACI.

Collins, M. P., et al. (2008). "An adequate theory for the shear strength of reinforced concrete structures." Magazine of Concrete Research **60**(9): 635-650.

Collins, M. P. and D. Kuchma (1999). "How safe are our large, lightly reinforced concrete beams, slabs, and footings?" ACI Structural Journal **96**(4).

Elzanaty, A. H., et al. (1986). Shear capacity of reinforced concrete beams using high-strength concrete. ACI Journal Proceedings, ACI.

Hofstetter, G. and G. Meschke (2011). Numerical Modeling of Concrete Cracking, Springer.

Johnson, M. K. and J. A. Ramirez (1989). "Minimum shear reinforcement in beams with higher strength concrete." ACI Structural Journal **86**(4).

Kani, G. (1964). The riddle of shear failure and its solution. ACI Journal Proceedings, ACI.

Kashif Shehzad, W. K., Khaliq-Ur-Rasheed Kiani (2014). "Shear Behaviour of Normal Strength Reinforced Concrete Slender Beams."

Kong, P. Y. and B. V. Rangan (1998). "Shear strength of high-performance concrete beams." ACI Structural Journal **95**(6).

Leonhardt, F. and R. Walther (1962). "Tests on Single Span Reinforced Concrete Beams with and without Web Reinforcement." Beton-und Stahlbetonbau: 37.

Leonhardt, F., et al. (1964). The Stuttgart shear tests, 1961: contributions to the treatment of the problems of shear in reinforced concrete construction.

MacGregor, J. G., et al. (1997). Reinforced concrete: mechanics and design, Prentice Hall Upper Saddle River, NJ.

Mörsch, E. (1910). Concrete-steel Construction:(Der Eisenbetonbau), Engineering news publishing Company.

Mphonde, A. G. and G. C. Frantz (1985). "Shear tests of high-and low-strength concrete beams with stirrups." ACI Special Publication **87**.

Placas, A. and P. E. Regan (1971). Shear failure of reinforced concrete beams. ACI Journal Proceedings, ACI.

Roller, J. J. and H. G. Russel (1990). "Shear strength of high-strength concrete beams with web reinforcement." ACI Structural Journal **87**(2).

Russo, G. and G. Zingone (1991). "Flexure-shear interaction model for longitudinally reinforced beams." ACI Structural Journal **88**(1).

Shioya, T., et al. (1985). Size effect on splitting tensile strength of concrete. Proceedings.

Swamy, R. and A. Andriopoulos (1974). "Contribution of aggregate interlock and dowel forces to the shear resistance of reinforced beams with web reinforcement." ACI Special Publication **42**.

Talbot, A. N. (1909). "Tests of reinforced concrete beams:: resistance to web stresses."

Yoon, Y.-S., et al. (1996). "Minimum shear reinforcement in normal, medium, and high-strength concrete beams." ACI Structural Journal **93**(5).

Zararis, P. D. (2003). "Shear Strength and Minimum Shear Reinforcement of Reinforced Concrete Slender Beams." ACI Structural Journal(Title no. 100-S22): 12.

Zararis, P. D. (2003). "Shear strength and minimum shear reinforcement of reinforced concrete slender beams." ACI Structural Journal **100**(2).

Zararis, P. D. and G. C. Papadakis (2001). "Diagonal shear failure and size effect in RC beams without web reinforcement." Journal of structural engineering **127**(7): 733-742.

Ziara, M. M. (1993). "The influence of confining the compression zone in the design of structural concrete beams."